Title: Single cell RNA-sequencing reveals no evidence for meiotic sex chromosome inactivation in the threespine stickleback fish

Short title: Lack of MSCI in threespine stickleback

Daniel E. Shaw, Wynter D. Ross, Alexis V. Lambert, and Michael A. White*

Department of Genetics, University of Georgia, Athens, GA, 30602

Corresponding Author:

Michael A. White

Department of Genetics, University of Georgia

120 Green St,

Athens, GA 30602

whitem@uga.edu

Abstract

Sex chromosomes often evolve unique patterns of gene expression during spermatogenesis. In many species, sex-linked genes are downregulated during meiosis in response to asynapsis of the heterogametic sex chromosome pair (meiotic sex chromosome inactivation; MSCI). This process has evolved convergently across many taxa with independently derived sex chromosomes. Our understanding how quickly MSCI can evolve and whether it is connected to the degree of sequence degeneration remains limited. Teleost fish are a noteworthy group to investigate MSCI because sex chromosomes have evolved repeatedly across species, often over short evolutionary timescales. Here, we investigate whether MSCI occurs in the threespine stickleback fish (*Gasterosteus aculeatus*), which have an X and Y chromosome that evolved less than 26 million years ago. Using single-cell RNA-seq, we found that the X and Y chromosomes do not have a signature of MSCI, maintaining gene expression across meiosis. Using immunofluorescence, we also show the threespine stickleback do not form a condensed sex body around the X and Y, a feature of MSCI in many species. We did not see patterns of gene content evolution documented in other species with MSCI. Y-linked ampliconic gene families were expressed across multiple stages of spermatogenesis, rather than being restricted to post-meiotic stages, like in mammals. Our work shows MSCI does not occur in the threespine stickleback fish and has not shaped the evolution of the Y chromosome. In addition, the absence of MSCI in the threespine stickleback suggests this process may not be a conserved feature of teleost fish, despite overall sequence degeneration and structural evolution of the Y chromosome, and argues for additional investigation in other species. We also observed testis-dependent differences in

coding and expression evolution for X-linked genes, revealing evidence of testis specific faster-X effect and gene-by-gene dosage compensation.

Author Summary

As male germ cells enter meiosis, the X and Y chromosome of many species undergo a drastic repression of gene expression. In mammals, this process has been shown to be essential for fertility, and the expression of sex-linked genes can lead to meiotic arrest and cell death. This process has only been studied in a handful of organisms, which limits our understanding how extensive MSCI is across the tree of life. Teleost fish are an understudied group with many examples of independently derived sex chromosomes across closely related species. Here, we investigate whether MSCI occurs in the threespine stickleback fish, using single-cell transcriptional profiling. We found gene expression remains active throughout meiosis on the sex chromosomes, indicating MSCI does not occur. This indicates that MSCI is not a conserved feature of all taxa and is not an inevitable outcome of degenerating Y chromosomes.

Introduction

Heteromorphic sex chromosomes often fail to fully synapse during meiosis due to a lack of sequence homology between the chromosome pair (i.e. X and Y or Z and W). In mammals, the X and Y chromosomes only synapse within the pseudoautosomal region, where all crossing over is restricted in males [1]. Outside of the pseudoautosomal region, the unsynapsed chromatin triggers a process of complete transcriptional silencing and sequestration into a dense sex body, known as meiotic sex chromosome inactivation (MSCI) [2-4]. Most genes remain silenced throughout post-meiotic stages [5, 6] MSCI may actually represent a more generalized process of

68 silencing of any unsynapsed chromosomes in male or female meiosis (MSUC; meiotic silencing
69 of unsynapsed chromatin) [7, 8]. Although the function of silencing remains unknown, it may
70 have a role in ensuring DNA double strand breaks are properly repaired during meiosis at
71 locations where chromosomes fail to synapse properly (reviewed in [3].

72 MSCI appears to have evolved independently in multiple lineages. In mammals, MSCI
73 evolved in the common ancestor of therians, approximately 180 million years ago after the origin
74 of the X and Y chromosomes [9]. Since their origin, the sex chromosomes have diverged
75 structurally in both marsupial and eutherian lineages, yet they still share many meiotic silencing
76 factors that initiate in response to the unpaired X and Y [10, 11]. Sex chromosomes
77 independently evolved within monotremes, and while a canonical sex body does not form [12],
78 gene expression is reduced drastically in the non-recombining region in platypus [13]. This
79 indicates a general mechanism for silencing unpaired chromosomes may have been present in the
80 common ancestor of all mammals. Outside of mammals, sex chromosome silencing occurs
81 across the hemizygous X chromosomes of *Caenorhabditis* species [14] and grasshoppers [15,
82 16], both of which have XO males, where the X lacks a pairing partner. Some evidence exists for
83 transcript repression from the X chromosome in the XY male germline of *Drosophila*
84 *melanogaster* [17-20], suggesting MSCI may also exist in this species (but also see [21, 22]).

85 MSCI imposes a strong selection pressure on the overall gene content of evolving sex
86 chromosomes. The X chromosome is a disfavored environment for genes with functions in
87 spermatogenesis if the X is transcriptionally silenced during meiosis [3]. One way to circumvent
88 silencing is to move genes from the suppressed sex chromosomes to the autosomes.
89 Retrotransposition of genes has been a major driver of gene content evolution on the mammalian
90 and *Drosophila* X chromosomes [23-25]. Another mechanism to circumvent transcriptional

91 suppression during meiosis may be to increase copy number of genes on the X chromosome to
92 produce more transcripts in spite of the repressive chromatin environment [3]. Many multi-copy
93 gene families on the mouse X chromosome are reactivated post-meiotically despite
94 chromosome-wide transcriptional silencing [26, 27]. Large multi-copy gene families also exist
95 on the mouse and bull Y chromosomes that have testis-specific gene expression and have roles in
96 spermatogenesis [28, 29]. Sex chromosomes have evolved repeatedly throughout the tree of life,
97 but outside of a few well-characterized species with relatively ancient sex chromosomes it
98 remains unclear the overall extent to which MSCI occurs and whether it is a common selection
99 pressure on sex-linked gene evolution.

100 The degree of synapsis between sex chromosomes can even vary in species where
101 substantial degeneration has occurred on the Y or W chromosomes. Birds have a ZW sex
102 chromosome system that evolved independently from mammals over 120 million years ago
103 [30]]. Similar to the mammalian Y chromosome, many species of bird W chromosomes share
104 little sequence homology with the Z chromosome [30]. Despite this, MSCI does not occur on the
105 ZW sex chromosomes [31]. In chickens, the heterologous Z and W chromosomes show complete
106 synapsis in a majority of pachytene oocytes [31]. Incomplete MSCI has also been shown within
107 mammals, where self-synapsis of the X chromosome in some spermatocytes blocks
108 transcriptional suppression of the chromosome [32]. Sex chromosomes with little sequence
109 divergence may also synapse more readily during meiosis, preventing MSCI. At the most
110 extreme, sex chromosomes that only differ at a small sex determination region may not interfere
111 with synapsis at all. For example, there is little sequence divergence between the X and Y
112 chromosome in the guppy [33-35], *Poecilia reticulata*, and these chromosomes fully pair with
113 each other during meiosis [36]. Additional focus on how different sex chromosomes achieve

114 pairing during meiosis is necessary to understand the extent of MSCI across convergently
115 evolving sex chromosomes.
116 The threespine stickleback fish *(Gasterosteus aculeatus)* is an excellent species to
117 explore whether MSCI occurs on a degenerating sex chromosome that fully synapses. The
118 threespine stickleback has an X and Y sex chromosome that evolved less than 26 million years
119 ago [37]. Since this time, the Y chromosome has diverged from the X chromosome at both the
120 sequence and structural level. The X and Y chromosomes have a 2.5 Mb pseudoautosomal
121 region, where all crossing over is restricted during meiosis [38]. The non-crossover region on the
122 Y chromosome has lost nearly half of the ancestral gene content [37, 39]. In addition, three
123 pericentric inversions have altered synteny between the X and Y [37, 40]. Despite this
124 degeneration, the sex chromosomes fully pair in a non-homologous fashion along their entire
125 chromosomal length during prophase I of meiosis [41]. Threespine stickleback provides a needed
126 perspective on the evolution of MSCI within teleost fish. Due to sex chromosome pairing in
127 meiosis, we hypothesized that MSCI would not occur during spermatogenesis and consequently
128 this process has not shaped the evolution of gene content on these chromosomes.
129 In this study, we used single-cell RNA sequencing to characterize sex-linked gene
130 expression throughout spermatogenesis. Consistent with full pairing and synapsis, we did not
131 find a stage-specific down regulation of X- or Y-linked genes across spermatogenesis. The sex
132 chromosomes were also not sequestered into a sex body. Our study indicates asynapsis and
133 MSCI is not an inevitable outcome for all degenerating sex chromosomes and argues for
134 additional research into other sex chromosome systems to understand why some heteromorphic
135 sex chromosomes can maintain synapsis despite a lack of sequence homology.
136

137 **Results**

138 **Identification of stickleback spermatogenic stages using single-cell RNA sequencing**

139 The testis is a highly heterogeneous organ and gene expression varies both spatially
140 across cell types as well as temporally across developmental stages [13, 42]. Spermatogenesis
141 occurs synchronously in the threespine stickleback [43]. At a given developmental stage, the
142 testes will be enriched for premeiotic, meiotic, or post-meiotic cells, along with somatic support
143 cells. In reproductively mature adult males, the testes will mostly contain mature sperm and
144 somatic cells. In order to capture all stages of spermatogenesis, we sequenced testes from lab-
145 reared males at different developmental stages. We sequenced 6147 cells from a single testis
146 dissected from an earlier stage of spermatogenesis and 2652 cells from a single testis dissected
147 from a male at a later stage of spermatogenesis. In order to maximize the total number of stages
148 of spermatogenesis, we also pooled the testes from two additional males from an intermediate
149 developmental stage (6027 cells total). The median number of genes detected were comparable
150 across samples (Testis sample 1: 271, Testis sample 2: 311, Testis sample 3: = 281), but sample
151 two had a higher number of genes and UMIs detected (Supplemental Figure 1), likely due to this
152 being the sample with lowest number of cells. Each testis sample cannot be treated as a direct
153 replicate of one another due to the differences in timing of synchronized spermatogenesis and
154 variation in the number of cells. However, we did find many replicated clusters, indicating
155 overlap in stages of spermatogenesis between the testis samples (Supplemental Figure 2).
156 Consistent with this, cells were hierarchically clustered by type rather than by sample, when
157 considering gene expression (Supplemental Figure 3). This suggests that batch effects on
158 expression level were minimal after integration and normalization. While we found similar cell
159 types across each sample, we found variation in the density of each cell type across samples. As

160 expected, we found a higher number of meiotic cells relative to post-meiotic cells, in the earliest
161 developmental sample (sample 1). However, some differences in cell population may also be due
162 to technical differences in sequencing library and UMI counts, as we also found less immune
163 cells in sample 1, which also had the lowest amount of UMIs detected. Among the three samples,
164 there were two unique cell clusters. Because these clusters were only present in a single sample,
165 we removed the cells (cluster 9 from sample 1, cluster 6 from sample 3) from all downstream
166 analyses. Non-replicated clusters could be due to rare cell populations only identified in one
167 sample or derived from batch differences between sequencing libraries [44].

168 To capture all stages of spermatogenesis in a single analysis, we merged the three
169 samples together and scaled gene expression accordingly. Between all of the samples, we
170 recovered a total of 12,136 cells after filtering. Clustering analysis revealed 15 distinct cell
171 clusters (Figure 1A). We identified 3,694 differentially expressed genes across all cell clusters
172 (Mann-Whitney U Test) (Supplemental File 1). Genes were considered differentially expressed
173 within a cluster if the gene was expressed in 25% of cells within the cluster, had a $\log_2$ fold
174 change > 0.25 for expression compared to all other clusters, and had a significantly different
175 level of expression evaluated with a P-value < 0.01 after correcting for multiple comparisons.
176 Among the differentially expressed genes, we identified those unique to cell-types in order to
177 assign spermatogenesis stages to each cluster.

178 Cell-type specific markers were identified from conserved genes expressed during
179 spermatogenesis from insects [45, 46], mammals [13, 42, 47-50], and other teleost fish [51-56].
180 Using these markers, we identified spermatogonia, spermatocytes, spermatids, and somatic cell
181 types (Table 1; Supplemental Figure 4). One class of somatic cells clustered separately from
182 spermatogenesis clusters and had differentially expressed genes that were not specific to testis

183 (i.e. *Hbae5*, *Rhag*; Cluster 11 and 12; Figure 1A). These were genes that are mostly expressed in
184 immune cells (e.g. monocytes and macrophages). We confirmed the expression of these markers
185 during spermatogenesis in other teleost species, including *Sebastes melanops* (black rockfish)
186 [55] and *Danio rerio* (zebrafish) [51]. These genes were also expressed in cells of the head
187 kidney, a hematopoietic organ with immune function in threespine stickleback [56].
188 A second group of somatic cells mapped distinctly from spermatogenesis cells, but also
189 had some expressed genes that were shared with some of the spermatogenesis clusters, consistent
190 with somatic cells of the testis (Sertoli and Leydig cells; Cluster 13; Figure 1A). The markers we
191 used to identify Sertoli and Leydig cells (e.g. *Gsdf* and *Fshr)* were also confirmed to be
192 expressed in zebrafish [51] and rockfish [55]. Within the differentially expressed genes, we
193 found several significantly enriched functions that corroborated our cell type assignment (Table
194 1).
195 For further analyses, we combined clusters into four major cell groups to explore
196 differences across major cell types: pre-meiotic, post-meiotic, meiotic, and somatic cells (Figure
197 1B and 1C). Within each of these broader categories, we found that gene expression levels were
198 highly correlated across each testis sample before integration (Spearman Rank Correlation R >
199 0.65 for all comparisons) (Supplemental Figure 5). We found the major cell type groups were
200 concordant between samples. The average gene expression of the 2000 highest expressed genes
201 in major cell types was highly correlated after normalization (mean rho of shared clusters =
202 0.83, all vs all clusters average rho = 0.36, Supplemental file 2).
203
204 **Sex-linked genes do not undergo meiotic silencing**

205 In mammals, genes within the non-recombining region of the sex chromosomes are not
206 transcribed (MSCI) [2, 3, 8]. To determine whether meiotic silencing has also evolved in
207 threespine stickleback fish, we compared rates of transcription between sex-linked and
208 autosomal genes for all genes expressed in that cell type. We found that gene expression was not
209 reduced on the X chromosome in meiotic cells, relative to somatic and pre-meiotic cell types
210 (Figure 2; $P > 0.05$). While the Y chromosome showed lower expression than the X
211 chromosome, Y-linked genes maintain similar levels of expression across pre-meiotic and
212 meiotic cells (Figure 2, $P > 0.05$). We also investigated whether MSCI was operating at a finer
213 scale within cell types or if this pattern was restricted to the four major cell groups. While we did
214 detect more variation in X:AA expression between cell types when analyzing each sample, likely
215 due to the smaller sample size of each cluster, we found that meiotic and post-meiotic expression
216 was not significantly lower than pre-meiotic expression in all three samples (Supplemental
217 Figure 6), indicating MSCI was also not operating in individual cell types.
218 MSCI could be restricted to certain classes of genes or regions of the sex chromosomes.
219 For example, testis-specific genes could be expressed higher, while housekeeping genes are
220 repressed. To test for this, we filtered out genes that appear to be exclusively expressed in testis
221 bulk RNA-seq compared to brain and liver [37, 39]. We found that broadly expressed genes are
222 also expressed across meiosis (Supplemental figure 7).We also examined whether there were
223 unique expression patterns among the differently aged evolutionary strata (Figure 3) [37]. We
224 found no evidence of silencing among the different regions of the sex chromosomes (Figure 3),
225 indicating this is not a phenomenon restricted to even the oldest stratum of the X and Y (stratum
226 1). Next, we repeated the analysis using a distinct clustering algorithm within Seurat, and by
227 clustering with a different software package (scanpy [57]). In both cases, we found that

228 normalized X expression was similar across cell types of spermatogenesis, regardless of cell
229 clustering approach and cell type annotation (Supplemental Figure 8). Overall, we found that
230 unlike mammals, chromosome-wide silencing does not occur on the threespine stickleback sex
231 chromosomes during meiosis.
232
233 **The threespine stickleback X and Y chromosomes are not condensed into a sex body**
234 During MSCI, the mammalian X and Y chromosomes are sequestered into a dense
235 structure, known as the sex body [2-4, 8]. A key marker of this structure are the phosphorylated
236 histone variant, γH2AX [2, 3, 6, 58]]. The threespine stickleback X and Y chromosomes likely
237 synapse fully and do not show evidence of delayed DSB repair [41]. Together with our results
238 that gene expression was not suppressed throughout meiosis, we predicted that a mammalian-like
239 MSCI sex body would also not be present during spermatogenesis. To test this, we characterized
240 how γH2AX accumulated throughout meiosis using immunofluorescence. γH2AX broadly
241 localized to all chromosomes beginning at leptotene in response to the initiation of DNA double
242 strand breaks [59] (Figure 4). During pachytene, double strand breaks are repaired and we
243 observed a concurrent reduction of γH2AX foci, similar to patterns observed in mammals [2].
244 However, at this stage we did not observe an aggregation of γH2AX synonymous with a sex
245 body (Figure 4). We staged a total of 146 nuclei from leptotene to pachytene. While, the X and Y
246 are not distinguishable at this resolution, none of the scored nuclei had any structure resembling
247 a sex body. This result is consistent with the expression data, supporting that canonical MSCI
248 does not occur in threespine stickleback fish due to the lack of asynapsis and sex body formation.
249
250 **Gene evolution on the sex chromosomes has not been shaped by MSCI**

251 Unique expression patterns can evolve rapidly on sex chromosomes [39, 60-64]. Sex
252 chromosomes can differentially accumulate pre- and post-meiotic genes [27, 65], gametologs can
253 gain testis-specific expression [66, 67], and Y-linked gametologs rapidly degenerate, losing
254 expression [68]. To explore this, we looked for enrichment of ancestral gametologs that were
255 only expressed from either the X or Y chromosome at different stages of spermatogenesis. We
256 found that pre- and post- meiotic cell types were over-enriched for Y-specific genes, while
257 meiotic cell types were under-enriched (Pre-meiotic: 2x, $P < 0.001$; Post-meiotic: 1.24x, $P =$
258 0.003; Meiotic: -3.15x, $P < 0.001$; Somatic: 1x, $P = 0.5$; hypergeometric test) (Supplemental
259 figure 9). We observed an over-enrichment of X-specific gametologs in pre-meiotic cell types,
260 but no other cell types were over- or under-enriched (pre-meiotic 1.39x, $P = 0.005$; meiotic:
261 1.16x, $P = 0.084$; post-meiotic: -1.13x, $P = 0.11$; somatic: 1.1x, $P = 0.290$; hypergeometric test)
262 (Supplemental figure 9). These results suggest early and late stages of spermatogenesis are prone
263 to the masculinization of gene expression, but not meiotic stages .
264 In addition to the ancestral complement of gametologs shared between the X and Y, the
265 Y chromosome has also acquired unique genes that originated from the autosomes [37]. After
266 translocation to the Y chromosome, many of these genes have further duplicated and evolved
267 testis-biased expression, suggesting a gain of spermatogenesis function [37]. In mammals, the
268 ancient Y chromosome has also accumulated species-specific gene duplicates that are enriched
269 for post-meiotic expression and have been speculated to be involved in intra-genomic conflicts
270 between X and Y bearing sperm during spermatogenesis [26, 28, 29, 69-71]. Due to the absence
271 of meiotic silencing in stickleback fish, we characterized how the expression of these Y-linked
272 duplicates compared to mammalian amplicons. We looked at the overall expression of all
273 paralogous copies within each gene family and assayed whether there were differences across the

274 four major cell types of spermatogenesis. We found that the Y-linked duplicated genes were
275 expressed across multiple cell types of spermatogenesis (Figure 5). Interestingly, in the absence
276 of chromosome wide silencing in meiosis, we found the highest number of expressed duplicate
277 families (104) in meiotic cell types, and expression for many duplicate families is highest in
278 meiosis compared to all other cell types (Figure 5). This was true for many genes, regardless of
279 the total number of paralogs, which ranged from 2-30 copies. This suggests that many amplicons
280 on the threespine stickleback Y chromosome may have functions throughout meiosis, rather than
281 post-meiotic stages as has been observed in mammals.

282 We searched for an enrichment of GO terms among the expressed duplicate genes to
283 assign function. We found that the predominant functions included chromatin assembly, DNA
284 packaging, and DNA repair. Specifically, we found many expressed duplicate families were
285 genes with critical functions in meiosis, including proteins involved in double strand break repair
286 (RAD proteins) and proteins involved in chromosome synapsis and segregation (SMC proteins)
287 [72]. Together, these results provide novel insight into the functions of duplicated Y-linked
288 genes, which in other species have been associated with post-meiotic expression [69, 70, 73].
289 Specifically, this finding highlights the role of meiotic functions in duplicated gene families
290 expressed on the Y, in the absence of meiotic silencing.

291 We searched for evidence of retrotransposition of genes throughout the genome, which
292 occurs at an increased frequency from the X chromosome in species with MSCI [17, 23, 74, 75].
293 Unlike these species, we did not find an excess of retrotransposition from the X chromosome in
294 the threespine stickleback. We identified nine examples of retrotransposition since the threespine
295 stickleback shared a common ancestor with the ninespine stickleback *(Pungitius pungitius)*
296 approximately 26 million years ago, before the threespine sex chromosomes evolved (the

297 ninespine stickleback has independently derived sex chromosomes) [76-78]. None of the nine
298 retrotransposition events were from the X chromosome. While nine total retrotransposition
299 events provides a low sample size to test for under-enrichment on the X chromosome, this trend
300 is much less pronounced than in humans and mice [73] Even though the threespine stickleback Y
301 chromosome shares many features of gene content evolution that have been observed on the
302 mammalian Y chromosome [37, 39], our results highlight that MSCI has not been a driving force
303 shaping these patterns.
304
305 **Genes expressed during spermatogenesis show signs of dosage compensation**
306 Many species have evolved mechanisms to compensate for the loss of expression from
307 the Y-linked allele [79]. However, threespine stickleback do not have evidence of chromosome-
308 wide mechanisms of dosage compensation in the heterogametic males, at least within brain tissue
309 analyzed in bulk [39]. It is possible that gene-by-gene dosage compensation has evolved and it
310 may be restricted to certain tissue or cell types. Indeed, the extent of chromosome-wide dosage
311 compensation has been shown to be variable across tissues [80-83]. To look for dosage
312 compensation during spermatogenesis, we compared normalized expression of X-linked genes
313 that still had a Y-linked allele (X+Y gametologs) with those where the Y-linked allele has been
314 lost (X-only gametologs). If dosage compensation is not occurring during spermatogenesis, we
315 would expect X-only gametologs to have expression levels half of what is observed globally
316 across autosomes. Instead, X-only gametologs had expression levels more similar to autosomes.
317 These X-only gametologs were also expressed significantly higher than X+Y gametologs in all
318 four major cell groups (Figure 6 ; $P < 0.01$). We compared this finding across the differentially
319 aged evolutionary strata of the sex chromosomes. If dosage compensation is occurring, we would

320 expect this effect would be strongest in the oldest evolutionary stratum (stratum 1), where the Y
321 chromosome has been degenerating for the greatest amount of time. Consistent with this, we
322 only detected a significant difference between X+Y gametologs and X-only gametologs for all
323 cell types in the oldest stratum (Stratum 1; $P < 0.01$) (Figure 6). This result is consistent with
324 previous findings that *cis*-regulatory elements in testis exhibited faster rates of sequence
325 divergence and positive selection on the X chromosome [65]. Our findings provide evidence that
326 sex-linked genes expressed during spermatogenesis may be dosage sensitive and have evolved
327 mechanisms to compensate for dosage loss from the Y chromosome.
328

329 **Genes have similar signatures of selection throughout stages of spermatogenesis despite**
330 **testis specific faster-X effect**

331 Sex chromosomes that have recently evolved are less likely to have signatures of a faster-
332 X effect [84], as XY shared genes are not hemizygous. Previous work in stickleback fish found
333 some evidence for a faster-X effect among hemizygous genes in the youngest strata [39].
334 However, this study used variants discovered from short-read sequencing and was additionally
335 limited by the lack of a reference threespine stickleback Y chromosome assembly and the lack of
336 a ninespine stickleback whole-genome assembly as an outgroup. Additionally, sex-linked genes
337 in the oldest part of the Y chromosome have been shown to be under purifying selection to
338 maintain dosage-sensitive genes [37, 39]. With improved genome resources now available, we
339 first wanted to test for evidence of different rates of coding evolution of sex-linked genes [37, 85,
340 86]. We identified all coding substitutions between threespine and ninespine stickleback, which
341 has an independently evolved sex chromosome pair on chromosome 12 [76]. We found similar
342 rates of non-synonymous to synonymous substitution rates (d_N/d_S) between autosomal genes and

343 all X-linked genes that are hemizygous . Y-linked hemizygous genes had a higher d_N/d_S than
344 autosomes, consistent with the degeneration of coding regions on this chromosome (
345 Supplemental Figure 10, P = 0.008). Interestingly, we found that X-linked gametologs that still
346 maintain a Y copy had lower d_N/d_S than autosomes (P < 0.001, Supplemental Figure 10). We
347 also observed a lower d_N/d_S than average for the X chromosome in the ninespine stickleback
348 (chromosome 12) (Supplemental Figure 11), suggesting X-linked gametologs are evolving
349 slower in both species. This is consistent with a recent theoretical model that proposed selection
350 is less efficient for gametologs on the X chromosome [83] (i.e. slower-X effect). Interestingly,
351 d_N/d_S of X-linked hemizygous genes was higher than autosomes, only for genes induced in major
352 cell groups of spermatogenesis, suggesting that the faster-X effect has affected male-specific
353 genes (Figure 7, P = 0.018, Kruskal-wallis and Dunn's test).
354 In other species, stages of spermatogenesis have different rates of coding evolution [13, 87-89].
355 In house mice, cell types in early stages are more evolutionarily constrained, while later stages
356 show signatures of rapid evolution, and this pattern is more extreme on the X chromosome due
357 to the faster X effect of highly degenerated Y chromosomes [88]. However, it remains unclear if
358 faster evolutionary rates would also apply to meiotic or post-meiotic genes on younger
359 chromosomes in the absence of meiotic silencing. We tested for differences in evolutionary rates
360 between genes induced across the four major cell groups of spermatogenesis. We found that
361 d_N/d_S was similar across all stages (Supplemental figure 12, P = 0.501, Kruskal Wallis test).
362 Together, this suggests evolutionary rates are similar across stages of stickleback
363 spermatogenesis.
364 **Discussion**

365 The repression of sex chromosomes during meiosis was first noted based on early
366 cytological evidence that many sex chromosomes were found in a condensed chromatin state
367 [90-92]. Condensation of the X chromosome was proposed to be a critical feature of
368 spermatogenesis, and could result in sterility if disrupted [90]. Since then, there have been many
369 hypotheses how the function of MSCI may improve the fidelity of meiosis including to help
370 avoid ectopic recombination, facilitate DSB repair, avoid expressing genes that have unrepaired
371 DSBs, or act as a meiotic checkpoint response [3, 91]. Molecular studies have revealed that
372 MSCI in mouse is initiated by the unsynaped state of the X and Y in male meiosis during the
373 pachytene stage and results in a complete lack of gene expression [2, 8]. Other hypotheses for
374 MSCI suggest it may be a result of how sex chromosome sequence evolves [93-95]. The
375 silencing of the X and Y may limit the effect of segregation distorters that would bias the
376 transmission of either chromosome during male meiosis [93]. The loss of spermatogenesis genes
377 on the X chromosome, perhaps through sexually antagonistic selection, may favor the
378 deactivation of the X during meiosis [94].
379 In this study, we found that the threespine stickleback X and Y chromosome maintain
380 relative expression of genes across all stages of spermatogenesis. Our findings align with
381 previous observations that the X and Y chromosomes fully pair during meiosis [41] . If the sex
382 chromosomes are fully associating in a non-homologous fashion, this would prevent MSCI from
383 occurring. In other species with heteromorphic sex chromosomes, full pairing has been shown to
384 occur despite an overall lack of homology between the chromosomes. Each documented case
385 thus far has revealed different mechanisms to achieve this. In the platypus, for instance, cohesins
386 (SMC3) differentially accumulate on the five X and five Y chromosomes during meiosis [96].
387 Although the exact function of the increased recruitment of cohesins to the sex chromosome

388 axial cores remains unknown [12, 96]. The threespine stickleback sex chromosomes do not
389 exhibit differential accumulation of SMC3 between the sex chromosomes and autosomes [41],
390 suggesting this is not required in all species for non-homologous pairing. In the chicken, the Z
391 chromosome undergoes synaptic adjustment to pair with the W [92]. This is followed by
392 assembly of the central element of the synaptonemal complex, indicating full synapsis of non-
393 homologous regions of the chromosomes [31, 97]. Consequently, MSCI does not occur [31].
394 Synaptic adjustment of the longer sex chromosome is also observed during pairing in the
395 threespine stickleback fish [41]. However, it remains unknown if full synapsis is also achieved
396 between the X and Y [41]. Both the X and Y chromosomes appear closely associated and
397 synapsed during prophase I of meiosis based on localization of the axial element, SMC3, but
398 without higher resolution microscopy, it cannot be ruled out that some regions are not fully
399 synapsed [41]. Additional work is necessary to understand if central element components, like
400 SYCP1, are also recruited during non-homologous pairing of the threespine stickleback X and Y
401 chromosomes and if full synapsis is required to prevent MSCI from occurring.
402 Alternatively, it is possible MSCI is not a conserved feature of all taxa and it does not
403 occur in stickleback fish. The initial finding that MSUC occurred in taxa as diverse as
404 *Neurospera crassa, C. elegans*, and mammals lead researchers to believe that MSCI may be
405 initiated in all species with divergent, heteromorphic sex chromosomes [98]. However, evidence
406 supporting the evolution of MSCI outside of the mammalian lineage has been somewhat
407 confounding. Despite some evidence of lower expression [97], the W and Z chromosome in
408 chicken oogenesis was found to largely maintain expression as the sex chromosomes maintain
409 non-homologous synapsis in female oocytes [31], perhaps through a similar mechanism of
410 synapsis as stickleback fish. In *Drosophila melanogaster*, some evidence suggests gene

411 expression is lowered on the X chromosome during meiosis [18, 99-101]. However, the extent of
412 silencing is less pronounced than mammals, does not occur on the Y, and may be an artifact of
413 the lack of dosage compensation in spermatocytes, or the movement of spermatocyte genes off
414 the X chromosome to avoid the lack of dosage compensation [22, 82, 83, 100]. Similar to our
415 findings in stickleback fish, the neo-sex chromosomes in *D. miranda* show no evidence of MSCI
416 [82]. Multiple insects have been reported to have silencing, including the grasshopper
417 (*Eyprepocnemis plorans*), which has complete silencing, independent of γH2AX accumulation
418 [102], and the mosquito (*Anopheles gambiae)* which has lower expression of the X chromosome,
419 though not all genes are silenced [103, 104]. This highlights a need for additional species to be
420 studied to understand the generalities of sex-linked gene expression during meiosis.

421 Teleost fish are one such understudied group. The existence of MSUC and MSCI remains
422 unclear and has only been investigated in a few species [105]. The swamp guppy (*Micropoecilia*
423 *picta*) has a degenerated Y chromosome relative to the X chromosome, yet cytological
424 investigations of meiosis revealed no presence of an obvious sex body that would indicate MSCI
425 [106]. If MSCI does not occur within teleost fish, the X and Y chromosomes of the threespine
426 stickleback would not need to fully synapse outside of the pseudoautosomal region and MSCI
427 would not be triggered. Future work in threespine stickleback should characterize the role of
428 RNA polymerase and repressive histone modifications, like H3K9me3, in regulating the sex
429 chromosomes during meiosis.

430 Chromosome-wide silencing creates strong constraints on sex-linked genes and inhibits
431 selfish genetic elements from being expressed in meiosis [93, 95, 107, 108]. Sex chromosomes
432 are suspected to be an evolutionary hotspot for the accumulation of selfish genetic elements that
433 can bias chromosomal transmission [95, 107, 108]. We found that X-linked hemizygous genes

434 expressed across all stages of spermatogenesis exhibited higher rates of protein coding evolution.
435 Our findings suggest that X-linked genes involved in spermatogenesis evolve faster than other
436 X-linked genes, evident by higher rates of coding evolution, and expression evolution related to
437 testis specific dosage compensation. Efficient selection of X-linked genes could lead to
438 intragenomic conflicts driven by selfishness between X- and Y- bearing sperm in this species.

439 Y chromosomes across many species have been found to accumulate gene duplications of
440 testis specific genes [28, 29, 37, 71, 109, 110]. Sex-linked gene amplification has been
441 hypothesized to be the result of selection pressure to escape the repressive environment of
442 silenced chromosomes. Genes escaping post-meiotic repression in mammals have been
443 putatively linked to transmission distortion [26-29, 73, 111, 112]. In the absence of MSCI in the
444 threespine stickleback, we observed that Y-linked duplicates were not enriched in post-meiotic
445 stages. Instead, amplified gene families were expressed throughout meiosis. Y-linked gene
446 duplications on the neo-Y chromosome of *Drosophila miranda* were also found to be expressed
447 during meiosis, rather than being restricted to post-meiotic cell types [82]. Therefore, it may be
448 possible that the enrichment of large ampliconic families explicitly related to post-meiotic
449 expression, may be restricted to mammalian lineages where repression of gene expression
450 extends beyond the meiotic stages of MSCI.

451 To date, no specific genes have been found to cause segregation distortion in threespine
452 stickleback fish, although two microsatellites have been found to have distorted transmission in
453 an F2 cross [113]. While most lab crosses yield 50:50 sex ratios, some wild populations have
454 been found to be female biased [114]. This could suggest that selection to repress conflicts to
455 maintain even sex ratios is ongoing. Similar to duplicated genes across mammals [29, 111] and
456 *Drosophila* [71, 109, 115], we did find that some duplicated gene families on the threespine

457 stickleback Y chromosome were also expressed in post-meiotic stages. Despite the lack of
458 repression in threespine stickleback, we identified several enriched categories of genes similar to
459 other species, including functions in chromatin assembly and maintenance. The well
460 characterized *Segregation Distorter* meiotic drive system in *Drosophila melanogaster*, distorts
461 transmission by manipulating chromatin state of other cells, leading to sperm dysfunction and
462 near-complete transmission of the *Sd* locus [116]. We also found an enrichment of genes
463 involved in DNA double strand break repair, including elements in the synaptonemal complex,
464 *Smc5.* Y-linked copies of this gene were expressed across both meiotic and post-meiotic stages.
465 Similarly, some of the ampliconic sex-linked gene families in *Mus musculus* (*Slx/Sly*) are
466 orthologs of another synaptonemal complex protein, SYCP3 [117]. Deletions and duplications of
467 *Slx* have been found to alter sex ratios in mice [26]. While the exact mechanisms of how these
468 genes affect transmission are unknown, the role of recombination proteins being duplicated and
469 neo-functionalized across independently derived Y chromosomes is intriguing. Functional testing
470 of the stickleback sex-linked genes may identify a similar role in transmission distortion.
471 Comparative work across multiple species has showed that several signatures of
472 spermatogenesis have evolved repeatedly, including the amplification of Y-linked
473 spermatogenesis genes, and meiotic/post-meiotic repression. While some features have evolved
474 convergently, many are not conserved across all species [3, 21, 31, 32] The vastly different
475 reproductive strategies and ecological factors affecting fish may alter some of the assumptions
476 made by classic conflict models proposed in mice and flies, and the absence of sex-linked
477 silencing in stickleback fish could be a result of having less selfishness in the male germline.
478 Most segregation distorter genes have been identified in species with internal fertilization like
479 mice and flies [116, 118, 119]. Externally fertilized eggs in fish could allow for increased male-

480 male competition [120], which may limit the pervasiveness of genomic conflict, due to the
481 deleterious effects on sperm production associated with selfishness [121]. However, reproductive
482 strategies can vary greatly across different species of fish. For example, male stickleback fish
483 court females by building nests, and then provide early stage paternal care by guarding clutches
484 of eggs laid by the female [122], though this behavior does not completely defend against other
485 males [123]. Broader comparisons across teleost fish would provide an interesting approach to
486 study these differences in a comparative framework, as there is variation in the types of mating
487 behaviors, reproductive strategies, and sex chromosomes, across closely related species.
488 Specifically, it would be noteworthy to compare the pervasiveness of male-male competition to
489 the rate of selfish evolution in spermatogenesis.
490
491
492 **Methods**
493 **Dissociation of testes for single-cell RNA sequencing**
494 Procedures using threespine stickleback fish were approved by the University of Georgia
495 Animal Care and Use Committee (protocol A2024 08-009-Y1-A0).
496 We performed three runs of single-cell RNA sequencing. Two runs were conducted with
497 a single male fish. The third run was a pool of males (see below). Each male was collected from
498 separate clutches of lab strains derived from wild-caught fish from Port Gardner Bay,
499 Washington. Individuals were selected based on age (~7 months), testis size, and testis
500 coloration, all of which are indicators that male fish are becoming reproductive and
501 spermatogenesis is proceeding. Stickleback fish have synchronous spermatogenesis. We
502 therefore aimed to select one male that was enriched for cells undergoing meiosis and one male

503 that was enriched for post-meiotic cells. The first male had slightly smaller and lighter colored
504 testes, consistent with earlier meiotic stages, while the second had larger, darker testes consistent
505 with later stages of testis maturation. We sequenced a third pool of two males as a replicate of
506 the first two sequencing runs. We identified two males with different testis coloration and size,
507 which were at different stages of spermatogenesis. Both males were seven-month-old fish
508 collected from separate clutches of fish derived from the same Port Gardner Bay population. We
509 pooled one testis from each male together for tissue dissociation and sequencing.

510 Cell dissociation was performed separately for each individual. Both testes from each
511 male were placed in ice cold PBS + 0.04% BSA. We followed a previously published single-cell
512 dissociation method used on mouse testes [47]. We first minced the tissue into small pieces
513 with McPherson-Vannas scissors in 200 µL of digestion medium (1mg/mL DNASE, 1mg/mL
514 collagenase/dispace, 1mg/ML hyaluronidase in solution of DMEM/F12). The cell solution was
515 incubated at 37º C for 10 minutes. The cells were filtered through a 40 µm cell strainer to obtain
516 a single-cell suspension, followed by centrifugation at 4º C, 400g for 10 minutes. The pelleted
517 cells were resuspended in 1mL of cold PBS + 0.04% BSA. Cell viability was assessed using
518 trypan blue. From the staining, we determined approximately 90% of the cells were viable. The
519 cells were immediately processed for sequencing using the 10x genomics single-cell sequencing
520 platform with 3' capture. 10X chromium and subsequent Illumina sequencing were both
521 performed at the Georgia Genome and Bioinformatics Core (University of Georgia).
522

523 **Processing of single-cell RNA-sequencing data**

524 The sequencing reads were demultiplexed with CellRanger (v 4.0.0) mkfastq with
525 bcl2fastq (Illumina) and default parameters. We ran CellRanger mkref on the threespine

526 stickleback genome assembly (v5.0) [37, 85]. We aligned fastq reads from all three samples
527 separately using CellRanger count with default parameters, plus the parameter --
528 chemistry=SC3Pv3. To filter for high quality cells, we used Seurat (v 4.0) to remove cells with >
529 3000 and <200 unique features (i.e. expressed transcripts) and cells with > 5% mitochondrial
530 counts. Cells with too many or too few identified features likely represent doublets or dead cells,
531 respectively. Transcript expression was normalized using Seurat (v4.0) scaledata, with default
532 parameters. After filtering each dataset separately, we merged all three sequencing runs using
533 Seurat merge, with default parameters. We then performed an analysis on the total dataset, first
534 by identifying cells from each dataset that are contained within nearest neighbors (anchors), by
535 running FindIntegrationAnchors with the dimensions set to dims = 1:20. Then we used Seurat
536 IntegrateData. This step defines a distance between datasets as the total number of cells in the
537 smaller dataset divided by the total number of anchors between each dataset, computes all
538 pairwise distances between each dataset, and clusters the distance matrix to determine a guide
539 tree. After the cells from each dataset were integrated, expression was scaled across each gene,
540 using scaledata. Finally, cells were reassigned to neighbors, clusters, and UMAP was run on the
541 complete dataset.
542
543 **Clustering and UMAP**
544 We followed the Seurat (v4.0) workflow [124] to perform cell clustering. We determined
545 dimensionality of the dataset by performing a jackstraw permutation in Seurat. Based on the
546 elbow plot and jackstraw plot (Supplemental Figure 13), we identified 20 significant principal
547 components for the integrated dataset with a $P < 0.001$. We ran Seurat findneighbors (Dims:1:12)
548 and Seurat findclusters (Resolution=0.8). Graph-based clustering is performed based on

549 construction of a nearest neighbor graph, and then applies a Leiden community detection
550 algorithm. The resolution factor is recommended to be between 0.4-1.2
551 (https://satijalab.org/seurat/articles/pbmc3k_tutorial.html). We experimented with a range of
552 values from 0.4-1.2 and found that the number of clusters from 0.8 was the most consistent with
553 marker identification and the total number of expected cell types in the threespine stickleback
554 testis [125, 126] To visualize the clusters, we ran the Seurat UMAP function set to 20
555 dimensions (Dims=1:20). We verified that most clusters had a similar number of reads per cell,
556 and expressed features per cell, to avoid identifying clusters based on read depth alone
557 (Supplemental Figure 14). We also performed alternative clustering approaches by rerunning
558 Seurat findcluster with the added parameter algorithm = Leiden. We then ran scanpy [57] on the
559 counts matrix using default parameters and a clustering resolution of 0.5.
560

561 **Identification of cell clusters**

562 Differentially expressed genes were identified using the FindAllMarkers function in
563 Seurat. A Mann-Whitney U test was used to compare gene expression of each gene across all
564 clusters to identify significantly different gene expression profiles between clusters. Genes were
565 considered differentially expressed between clusters if there was a p-value < 0.001 after
566 correcting for multiple comparisons based on a Bonferroni correction. To relate cell clusters to
567 known cell types, we identified upregulated genes specific to clusters that were well
568 characterized genes from mammals [13, 42, 47-50, 127] and fish [51-55].
569

570 **Gene ontology**

571 We used the ShinyGO v0.741 web-based tool to identify gene ontology of upregulated
572 genes for each cluster with the genome set to "Stickleback" and processes set to "All available
573 gene sets." We used all stickleback genes expressed in our single-cell RNA dataset as the
574 background, to identify enrichment of biological processes involved in the significantly up-
575 regulated genes of each cluster. For each set of genes, we calculated the fold enrichment of genes
576 within a pathway and a false discovery rate (FDR). We only retained GO terms with an FDR <
577 0.01.
578
579 **Gene expression across the sex chromosomes**
580 To analyze chromosome-wide expression patterns across cells within a cluster, we
581 extracted alignments from each cluster output using pysam (v 0.16.0.1) and a custom python
582 script (https://github.com/daniel-shaw1/Single-Cell-RNA-
583 sequencing/blob/main/Split_bam_by_cluster.py), that separates RNA alignments for each
584 cluster. The separation of alignment files was run separately for each of the three independent
585 samples based on CellRanger clustering. We counted the total number of reads that aligned
586 within genes for each cluster using htseq-count (v 0.13.5) (-mode union --nonunique all --
587 minaqual 1 –stranded=no) [128]. These parameters were previously used to identify expression
588 of Y-linked genes in threespine stickleback with bulk RNA-seq [37]. We counted reads within
589 genes of the Y chromosome from published annotations [37] as well as within genes on the
590 autosomes and X chromosome, using annotations from Ensembl (build 107) [129] (Y genes in
591 Supplemental File 2). Reads were counted across the entire transcript as one feature. For both
592 sex chromosomes, we retained all genes with at least a count of one. To assess how gene
593 expression changes on the X and Y chromosomes relative to autosomes across spermatogenesis,

594 we normalized the total expression of each gene on the X and Y by the median expression of all
595 genes across the autosomes of each cluster and then cluster counts were averaged into four
596 categories for each major stage (i.e. somatic, pre-meiotic, meiotic, or post-meiotic).
597 We also assayed gene expression of duplicate gene families across the Y chromosome
598 that were previously annotated [37]. To analyze the overall expression level of each duplicate
599 gene family, we counted the total number of reads that aligned to each paralog within the family
600 and then summed these counts across all paralogs to get an overall count for each duplicate gene
601 family. We normalized counts for each duplicate gene family per cluster by dividing by the
602 library size of each cluster. Normalized gene duplicate expression was plotted using Morpheus
603 (https://software.broadinstitute.org/morpheus.)
604 We used previously published bulk RNA-seq from brain [39] (NCBI
605 BioProject PRJNA277770), liver [37] (NCBI BioProject PRJNA591630), and testis [37] (NCBI
606 BioProject PRJNA591630) to identify testis-specific genes expressed from the sex chromosomes
607 in order to distinguish them from genes that were broadly expressed across multiple organs. We
608 aligned three replicates of RNA-seq reads as previously described [66], and identified all of the
609 genes that were only expressed in testis. Genes were considered expressed if they had a read
610 count greater than one.
611 For identifying allele specific genes in Supplemental Figure 9, we used the full set of sex-
612 linked genes expressed in the testis to confirm allele specific expression of X- and Y- linked
613 genes. We identified all genes that had transcripts aligned to only one sex chromosome in a
614 major cell group in the scRNA-seq, then, we verified mono-allelic expression of those genes in
615 bulk RNA-seq testis to identify a conservative list of mono-allelically expressed genes.
616

617 **Detection of retrotransposition throughout the genome**

618 We searched for evidence of retrotransposition of genes from the autosomes and the X
619 chromosome. We aligned all protein coding sequences from the threespine stickleback (NCBI
620 release 100) to the threespine stickleback genome assembly (v. 5) [85]. In order to identify
621 putative retrotranspositions unique to the threespine stickleback lineage after the X and Y
622 chromosomes evolved, we also aligned the threespine stickleback protein coding sequences to an
623 outgroup species, the ninespine stickleback (v. 2.1 genome) [86]. We aligned all protein
624 sequences using Exonerate (v. 2.4) with parameters --model protein2genome --cores 8 --bestn 5 -
625 -showalignment FALSE --showvulgar TRUE --ryo "%ps\\n" [130]. We searched for protein
626 sequences that had greater than or equal to one intron that aligned to a second location in the
627 threespine genome with zero introns. These putative retrotranspositions were confirmed to be
628 specific to the threespine stickleback by verifying the alignment did not exist on the orthologous
629 autosome of the ninespine stickleback.

630

631 **Protein coding divergence**

632 In order to compare coding sequence evolution, we aligned the ninespine stickleback fish
633 CDS (NCBI NSP_V7) to the threespine stickleback genome [85] using Exonerate (v. 2.4)
634 (exonerate --model est2genome -M 2000 --bestn 15 --percent 25) [130]**.** We ran codeml from the
635 PAML (phylogenetic analysis by maximum likelihood) (runmode =-2) software package [131] to
636 calculate d_N, d_S, and d_N/d_S for all alignable coding sequence between the threespine and
637 ninespine stickleback. Exonerate alignments were filtered to remove stop codons and gaps, and
638 processed into a codeml compatible input using a custom Perl script (https://github.com/daniel-
639 shaw1/Single-Cell-RNA-sequencing), modified from a previous study [37]. For genes with

640 multiple annotated transcripts that aligned between the threespine and ninespine stickleback,
641 d_N/d_S ratios were averaged across the transcripts. Genes with a d_N/d_S value of 99 were removed
642 as these values are unreliable and occur when a gene does not have synonymous substitutions.
643 For genes with a d_N/d_S estimate, we identified genes that had higher expression in one of the
644 major cell types if they had 2x the expression of the median number of counts across the other
645 three groups. These counts were found using a custom R script (https://github.com/daniel-
646 shaw1/Single-Cell-RNA-sequencing/blob/main/induced_dnds.r.)
647

648 **Meiotic chromosome spreads**

649 The methods used for chromosome spreads were adapted from a protocol for zebrafish
650 [132]. We collected fish that were undergoing meiosis that were five to eight months in age and
651 had minimal pigmentation of the testes [41]. Whole testes were removed and submerged in 1 mL
652 of 1X PBS inside a 1 mL Douce homogenizer. The tissue was homogenized by grinding with the
653 tight pestle approximately 10 times. The entire volume of cell suspension was transferred to a 1.6
654 mL tube and centrifuged at 500 xg for five minutes. The supernatant was then removed and the
655 pellet was resuspended in 600 µL of 0.8% sodium citrate. The volume of sodium citrate was
656 adjusted based on the size of the pellet to achieve a low turbidity solution. The sodium citrate
657 cell suspension was incubated at room temperature for five to eight minutes. 20 µL of the cell
658 suspension and 20 µL of 100mM sucrose was pipetted onto each slide and spread by gently
659 tilting the slide. 100 µL of 1% (pH 8.5, adjusted with 0.1 M sodium tetraborate)
660 paraformaldehyde solution with 0.15% TX-100 was then added and spread across each slide
661 before incubating in a humid chamber at room temperature for two and a half hours. After
662 incubating the slides, we removed the top of the humid chamber to cure the slides overnight.

663 After curing, the slides were washed 3 consecutive times for 15, five, and five minutes in 1X
664 PBS with gentle agitation. Slides were allowed to dry for 15-20 minutes before
665 immunofluorescence or storing at –20°C.
666
667 **Immunofluorescence staining of SMC3 and γH2AX**
668 1.5 mL of permeabilization solution (1X PBS, 1 mM EDTA, and 1% TritonX-100) was
669 pipetted onto the slides and incubated for 20 minutes at room temperature. After dumping off the
670 solution, the slides were blocked with 1.5 mL of 1X antibody dilution buffer, incubating at room
671 temperature for 30 minutes. A 1:80 dilution of primary antibodies in 40 µL total volume was
672 pipetted on each slide (anti-SMC3, Abcam ab9263; anti- γH2AX, DSHB UNC93-5.2.1). The
673 slides were sealed with coverslips and rubber cement before being incubated in a humid chamber
674 overnight at 4°C. After incubating overnight, the coverslips were allowed to float off in 1X PBS,
675 and the slides were blocked with 1.5 mL 1X antibody dilution buffer for 30 minutes at room
676 temperature. A 1:100 dilution of secondary antibodies in 40 µL total volume was pipetted on
677 each slide (goat anti-rabbit Alexa Fluor 488, Abcam ab150077; goat anti-mouse Alexa 568,
678 ThermoFisher A-21134). The slides were sealed with coverslips and rubber cement before
679 incubating in a humid chamber at 37°C for two to three hours. After the coverslips were
680 removed, the slides were washed three times for 15, five and five minutes in 1X PBS with gentle
681 agitation. 40 µL of Vectashield Antifade Mounting Media with DAPI (Vector Labs) was added
682 to the slides and sealed with coverslips and nail polish.
683
684 **Staging of Meiocytes and Super Resolution Imaging**

685 The chromosome spreads were viewed and staged with a Nikon Eclipse Ti2 Microscope
686 with a 100x oil immersion lens. Prophase I stages were identified with the following criteria:
687 small, non-contiguous stretches of SMC3 were defined as leptotene; long SMC3 pieces and
688 incomplete strands indicating an absence of synapsis were defined as zygotene; and pachytene
689 was identified by fully formed SMC3 strands, suggesting complete synapsis. Final images were
690 taken with a Zeiss Elyra S1 (SR-SIM) Super Resolution Microscope with 100x oil immersion
691 lens. The images were processed with ImageJ and Zeiss Black software.
692

693 **Data availability**

694 The single cell data for this manuscript is available within the short reads archive under
695 PRJNA1191497. The Bulk RNA-seq is previously published and available on the short reads
696 archive: Brain: PRJNA277770, Liver: PRJNA591630, Testis: PRJNA591630.
697 Scripts and bioinformatic pipelines are available at: https://github.com/daniel-shaw1/Single-
698 Cell-RNA-sequencing
699 All microscopy images are available upon request.
700

701 **Acknowledgements**

702 This work was supported by the National Science Foundation MCB 1943283 (M.A.W.), the
703 National Institutes of Health R01GM147312 (M.A.W.), the University of Georgia Research
704 Foundation (D.E.S.), and by the Society for Study of Evolution R.C. Lewontin Early Award
705 (D.E.S). Single cell library preparations and sequencing were performed at the UGA Georgia
706 Genome and Bioinformatics Core.
707

708 **Declaration of interests**

709 The authors declare no conflicts of interests.

710 **Figures**

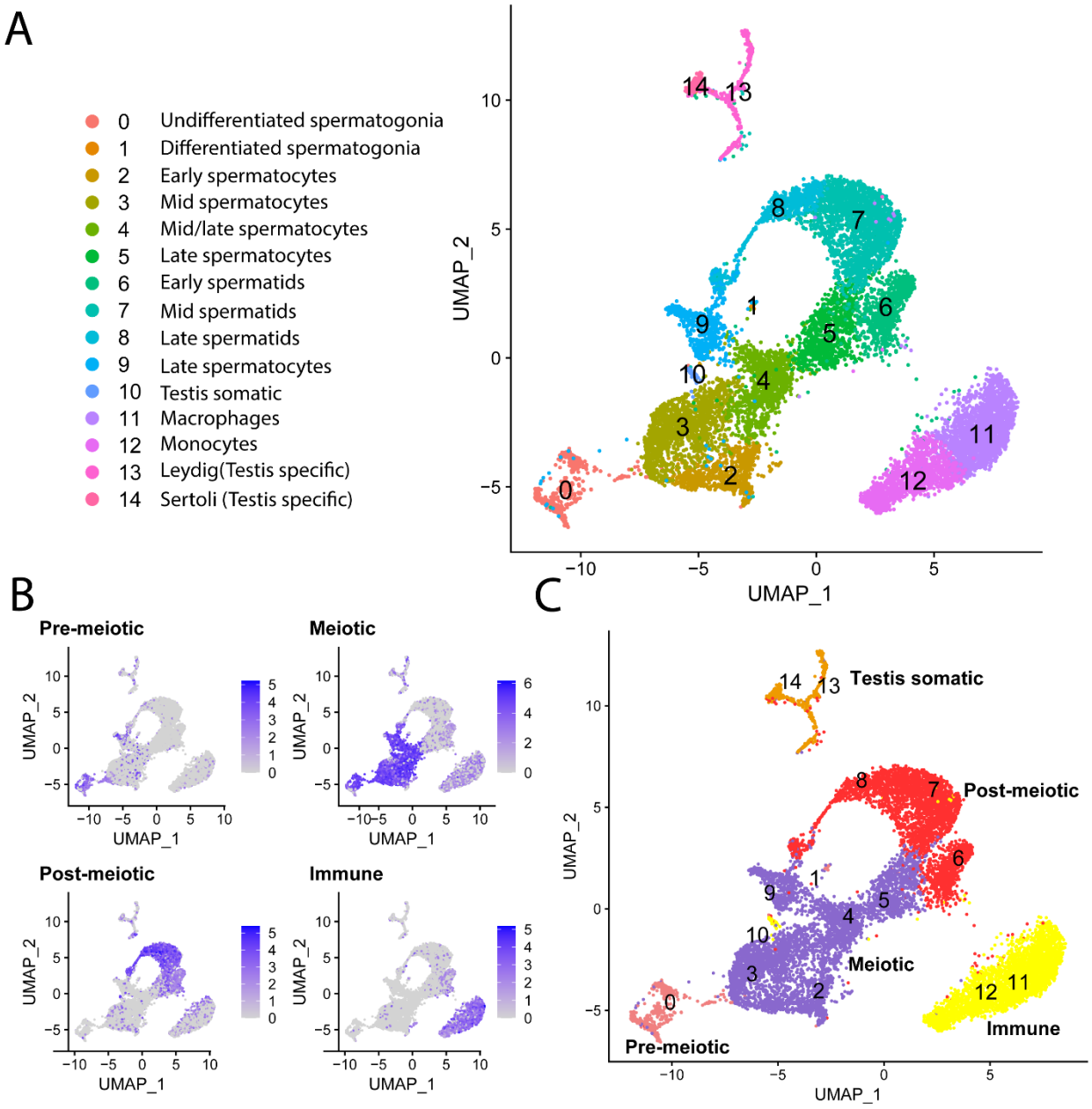

711

712 **Figure 1. Single-cell RNA-seq of threespine stickleback spermatogenesis.** Identified clusters

713 of pre-meiotic, meiotic, post-meiotic, and somatic cell populations integrated from three

714 sequencing runs. (**A**) Visualization of single-cell expression profiles of spermatogenesis in

715 UMAP projection. We identified 15 clusters and related them to stages of spermatogenesis based

716 on significantly upregulated marker genes and GO terms (Table 1). (**B**) Examples of enrichment

717 of key marker genes across the four main stages of spermatogenesis. Additional marker genes

718 are in Table 1. (**C**) The four main spermatogenesis stages overlaid on the UMAP projection.

719

720

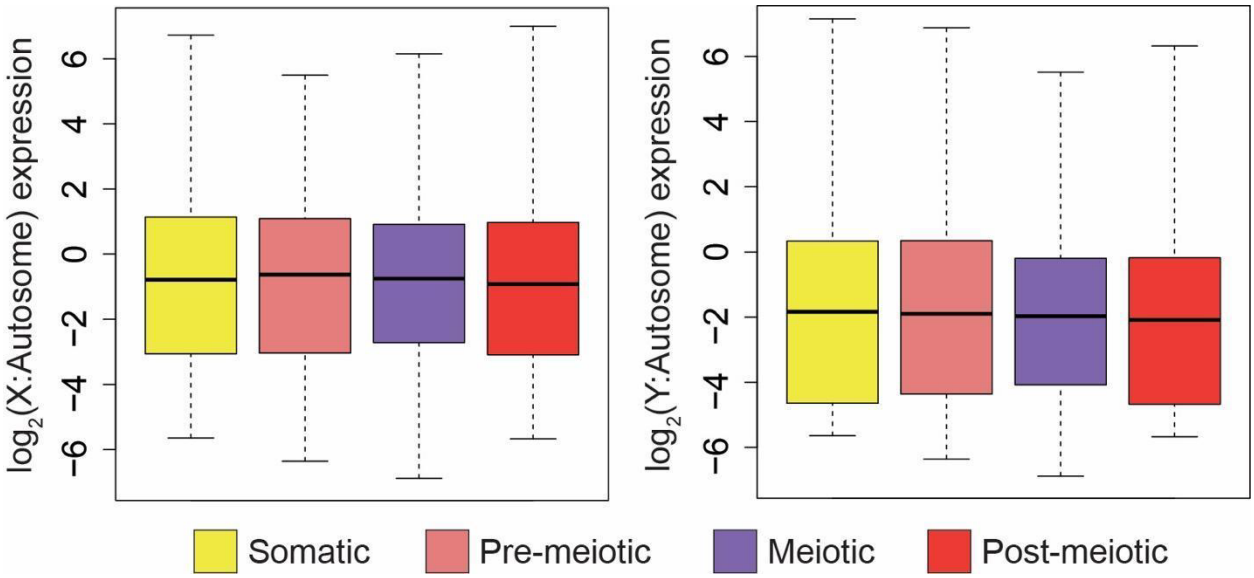

721

722 **Figure 2. Sex-linked gene expression does not change throughout spermatogenesis**. X- and

723 Y-linked gene expression was normalized to median autosome expression level for each stage of

724 spermatogenesis. Relative to median autosome expression, X- (left) and Y-linked (right) gene

725 expression does not change across stages of spermatogenesis. (Pairwise Mann-Whitney U Test, P

726 > 0.05). Outliers are not shown. Pre-meiotic X: N = 500 , Meiotic X: N = 506, Post-meiotic X:

727 N = 534, Somatic X: = 524. Pre-meiotic Y: N= 442, Meiotic Y: N = 468, Post-meiotic Y: N =

728 442, Somatic Y: N = 410. Analysis excludes clusters 6 and 9 due to lack of replication between

729 samples.

730

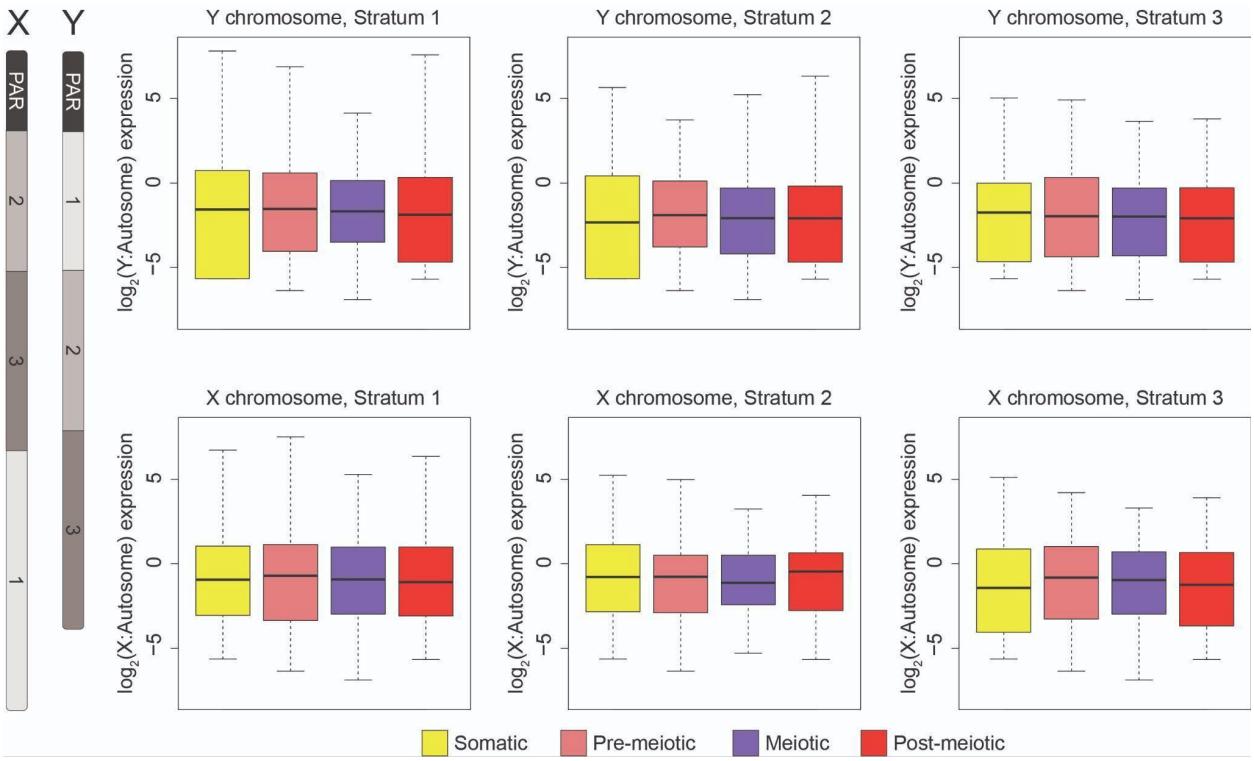

Figure 3. Sex-linked gene expression does not change throughout spermatogenesis in each of the evolutionary strata.

The sex chromosomes contain three distinct evolutionary strata at different states of divergence formed by nested inversions (left). Sex-linked gene expression does not change across spermatogenesis in the three different evolutionary strata. X- and Y-linked gene expression was normalized to median autosome expression level for each stage of spermatogenesis. Relative to median autosome expression, X- (bottom) and Y-linked (top) gene expression does not change throughout spermatogenesis in each of the three strata (stratum 1: oldest, stratum 2: middle, stratum 3: youngest; Pairwise Mann-Whitney U Test, $P > 0.05$). The recombining pseudoautosomal region (PAR) is indicated for reference. Outliers are not shown.

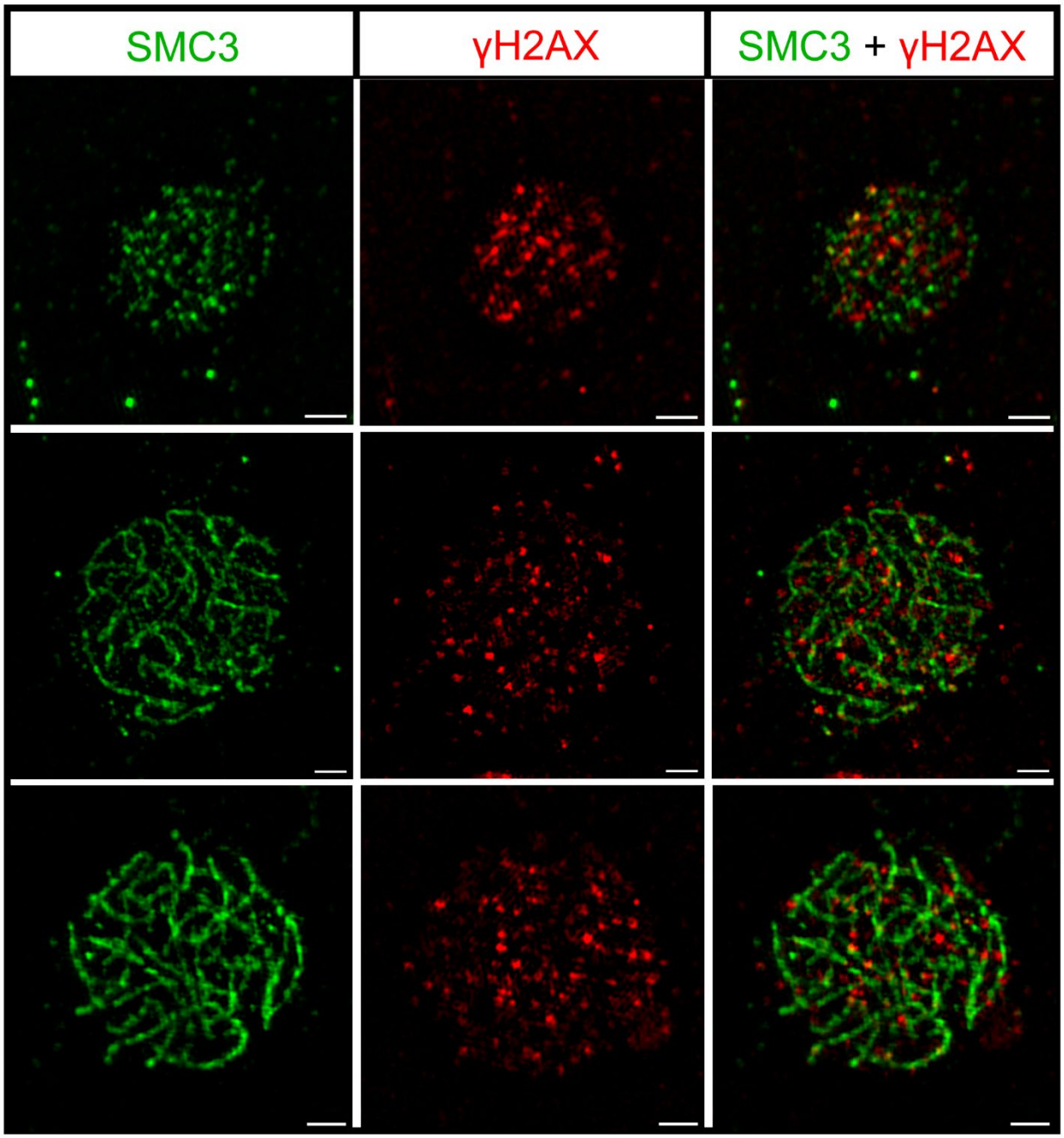

743

744 **Figure 4. The X and Y chromosomes are not sequestered into a sex body**. The highest
745 density of the phosphorylated histone variant, γH2AX, a marker of DNA damage (red) occurs
746 during leptotene (top), when the greatest number of DNA double strand breaks also occur.
747 γH2AX localization decreases as double strand breaks are repaired in zygotene (middle) and
748 pachytene (bottom). The sex chromosomes are repaired at the same rate since they are not

749 sequestered into a dense, γH2AX containing sex body at pachytene. The synaptonemal complex

750 axes are immunolabeled against the axial protein, SMC3 (green). The scale bar is 5 µm.

751

752

753

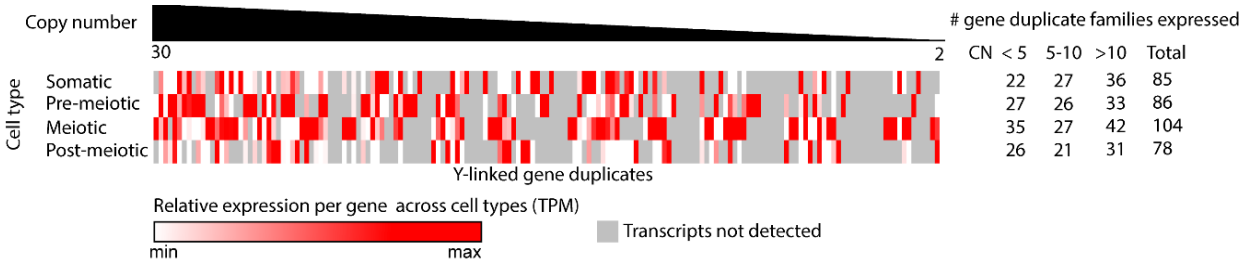

754

755 **Figure 5. Y-linked duplicate gene families are expressed across stages of spermatogenesis.**

756 Duplicate gene families on the Y chromosome are enriched for expression during

757 spermatogenesis. The greatest number of duplicate families were found to be expressed in

758 meiotic cell types. Normalized counts for all paralogous copies of a gene family were summed to

759 determine an aggregate expression level.

760

761

762

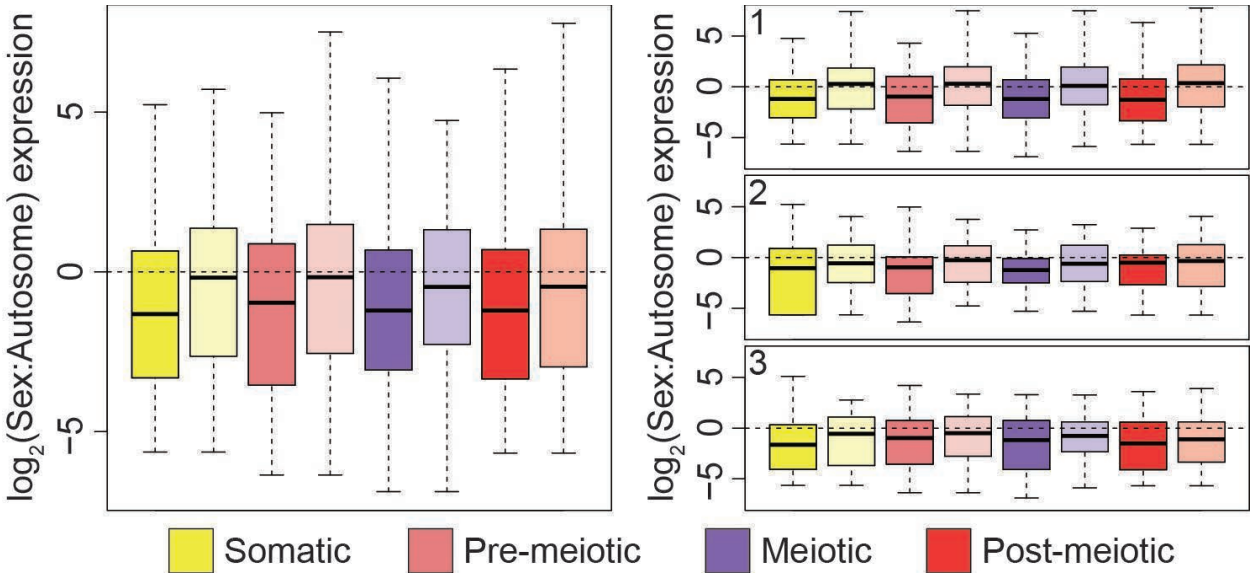

Figure 6. Spermatogenesis genes that have lost a Y-linked allele are dosage compensated. Genes with alleles on both the X and Y chromosomes (X+Y gametologs; dark shades) have lower expression relative to autosomes than genes that only have an X-linked allele (X-only gametologs; lighter shades). This indicates the X-only gametologs are upregulated to more closely match median autosome expression levels. All X-only genes are significantly higher than X+Y gametologs for all cell types (somatic: P = 0.004; pre-meiotic: P = 0.008; meiotic: P= 0.015; post-meiotic: P = 0.037; Kruskal-Wallis and Dunn's test.). When separated by the three evolutionary strata (right panels), X-only genes are expressed higher for all cell types in stratum 1 (the oldest region). X-only genes and X+Y gametologs are not significantly different for strata 2 and 3 (the two youngest regions) across all cell types (stratum 1 somatic: P = 0.001; stratum 1 pre-meiotic: P = 0.007; stratum 1 meiotic: P= 0.012; stratum 1 post-meiotic: P = 0.004; stratum 2 somatic: P = 0.301; stratum 2 re-meiotic: P=0.124; stratum 2 meiotic: P = 0.31; stratum 2 post-meiotic: P = 0.391; stratum 3 somatic: P = 0.115; stratum 3 pre-meiotic: P = 0.34; stratum 3 meiotic: P = 0.302; stratum 3 post-meiotic: P = 0.632; Kruskal-Wallis and Dunn's test). Outliers are not shown.

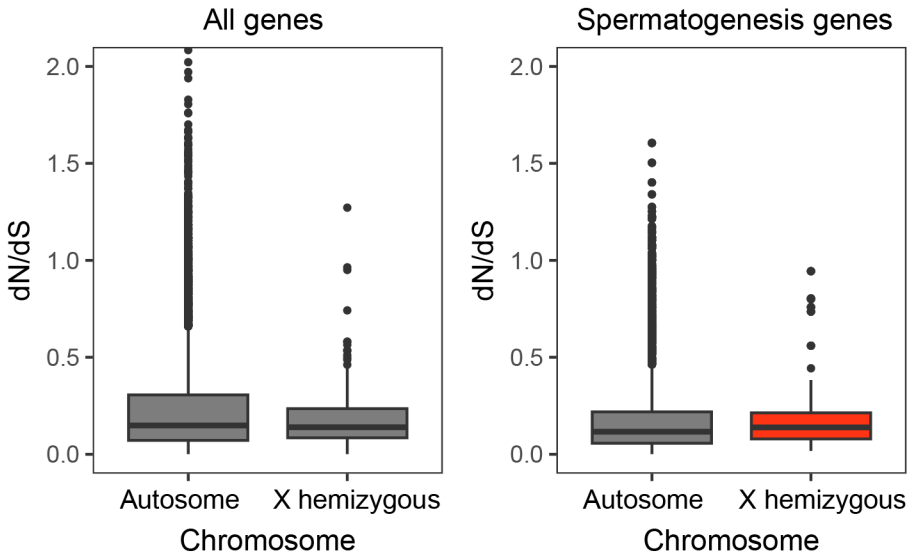

Figure 7. The faster-X effect is specific to spermatogenesis genes. Non-synonymous and synonymous substitutions were quantified between the threespine and ninespine stickleback fish, for 11,493 genes. X hemizygous genes have similar d_N/d_S as autosomes for all genes. For genes induced in spermatogenesis (N = 2378), X hemizygous genes have higher d_N/d_S than induced genes on autosomes (P = 0.018, Mann-Whitney U test, see Supplemental Figure 11 for all comparisons). Genes were defined as induced if they had expression levels greater than 2x the median expression in any major cell group in spermatogenesis.

Tables

Table 1. Representative marker genes and gene ontology functions enriched in each cell type.

794

795

796

Cluster identification	Characterization	Representative spermatogenic-related markers identified in cluster (P < 0.01)	Relevant GO terms (FDR < 0.01)
Early Spermatogonia	Undifferentiation, maintenance	*id4, npsn, ptpn6, myh9a, ctss2.1 hcls1, ponzr1, coro1a, itgb2, scinlb*	cell homeostasis, cell number homeostasis, NADP metabolic process
Late Spermatogonia	Differentiating, cell proliferation, hormones	*gata6, id1, ar, grnb, ptn, cyc1, prdx3, ctsa, h2ax*	Differentiation, chromosome, cell cycle
Early Spermatocytes	Early prophase, DSB formation	*smc2b, smc1al,hells, rab5c,rab35b,cbx3a, NASP,tex11*	core histone, centromere kinetochore, tubulin, ribosomal
Mid spermatocytes	Late prophase, DSB processing and strand invasion	*rad51, rad54, meig1, ccna1, map2k6,akirin2, cdk9, mns1, dyrk2, ccnb1*	embryo development, cell cycle, regulation of cell cycle, recombination
Mid-Late spermatocytes	Late meiosis, spindle assembly	*smc3, rab24, cenpv, cetn2,dnal1,cbx8b,rab8a,spag1,mospd1,cdc37*	chromosome organization, condensed chromosome, centromere, chromosome segregation, spindle
Late spermatocytes	Late meiosis, segregation and cell division	*cbx1, caprin1a, ccnb2, cfap57, SMARCA5, cdca8,rad23b, smc4,ncapd2,spata18,nusap1, fzr1a*	Sister chromatid segregation, cell cycle, cilium organization, nuclear division, organelle fission, kinetochore
Early Spermatids	Spermiogenesis	*ak1, taf9, ybx1,map6a, dctn3*	Cilium, motile cilium, dynein complex, centriole
Late spermatid	Sperm maturation	*gapdh, gapdhs, krt18a.1, arpc3, myh9b*	Axoneme assembly, axoneme, ciliary plasm
Testis somatic	Sertoli, leydig	*Gsdf, klf6a, coro1ca, ca8, fosab, fshr*	Hormone biosynthesis, Sertoli cell development
Immune cells	Monocytes, Macrophages, blood	*HBE1, mibp2, hbae5, rhag, cat, tob1a*	erythrocyte development, immune system development

797

798

References

1. Ellis N, Goodfellow PN. The mammalian pseudoautosomal region. Trends in Genetics. 1989;5:406-10. doi: https://doi.org/10.1016/0168-9525(89)90199-6.
2. Turner JMA. Meiotic sex chromosome inactivation. Development. 2007;134(10):1823-31. doi: 10.1242/dev.000018.
3. Turner JMA. Meiotic Silencing in Mammals. Annual Review of Genetics. 2015;49(1):395-412. doi: 10.1146/annurev-genet-112414-055145.
4. Handel MA. The XY body: a specialized meiotic chromatin domain. Exp Cell Res. 2004;296(1):57-63. Epub 2004/05/04. doi: 10.1016/j.yexcr.2004.03.008. PubMed PMID: 15120994.
5. Namekawa SH, Park PJ, Zhang L-F, Shima JE, McCarrey JR, Griswold MD, et al. Postmeiotic Sex Chromatin in the Male Germline of Mice. Current Biology. 2006;16(7):660-7. doi: 10.1016/j.cub.2006.01.066.
6. Turner JMA, Mahadevaiah SK, Ellis PJI, Mitchell MJ, Burgoyne PS. Pachytene Asynapsis Drives Meiotic Sex Chromosome Inactivation and Leads to Substantial Postmeiotic Repression in Spermatids. Developmental Cell. 2006;10(4):521-9. doi: 10.1016/j.devcel.2006.02.009.
7. Shiu PK, Raju NB, Zickler D, Metzenberg RL. Meiotic silencing by unpaired DNA. Cell. 2001;107(7):905-16. Epub 2002/01/10. doi: 10.1016/s0092-8674(01)00609-2. PubMed PMID: 11779466.
8. Turner JM, Mahadevaiah SK, Fernandez-Capetillo O, Nussenzweig A, Xu X, Deng CX, et al. Silencing of unsynapsed meiotic chromosomes in the mouse. Nat Genet. 2005;37(1):41-7. Epub 2004/12/08. doi: 10.1038/ng1484. PubMed PMID: 15580272.
9. Cortez D, Marin R, Toledo-Flores D, Froidevaux L, Liechti A, Waters PD, et al. Origins and functional evolution of Y chromosomes across mammals. Nature. 2014;508(7497):488-93. doi: 10.1038/nature13151.
10. Franco MJ, Sciurano RB, Solari AJ. Protein immunolocalization supports the presence of identical mechanisms of XY body formation in eutherians and marsupials. Chromosome Research. 2007;15(6):815-24. doi: 10.1007/s10577-007-1165-7.
11. Namekawa SH, Vandeberg JL, McCarrey JR, Lee JT. Sex chromosome silencing in the marsupial male germ line. Proceedings of the National Academy of Sciences. 2007;104(23):9730-5. doi: 10.1073/pnas.0700323104.
12. Daish TJ, Casey AE, Grutzner F. Lack of sex chromosome specific meiotic silencing in platypus reveals origin of MSCI in therian mammals. BMC Biology. 2015;13(1). doi: 10.1186/s12915-015-0215-4.
13. Murat F, Mbengue N, Winge SB, Trefzer T, Leushkin E, Sepp M, et al. The molecular evolution of spermatogenesis across mammals. Nature. 2023;613(7943):308-16. doi: 10.1038/s41586-022-05547-7.
14. Larson BJ, Van MV, Nakayama T, Engebrecht J. Plasticity in the Meiotic Epigenetic Landscape of Sex Chromosomes in Caenorhabditis Species. Genetics. 2016;203(4):1641-58. doi: 10.1534/genetics.116.191130.
15. Cabrero J, Teruel M, Carmona FD, Camacho JP. Histone H2AX phosphorylation is associated with most meiotic events in grasshopper. Cytogenet Genome Res. 2007;116(4):311-5. Epub 2007/04/14. doi: 10.1159/000100416. PubMed PMID: 17431330.

842 16. Cabrero J, Teruel M, Carmona FD, Jiménez R, Camacho JP. Histone H3 lysine 9
843 acetylation pattern suggests that X and B chromosomes are silenced during entire male meiosis
844 in a grasshopper. Cytogenet Genome Res. 2007;119(1-2):135-42. Epub 2007/12/28. doi:
845 10.1159/000109630. PubMed PMID: 18160793.
846 17. Vibranovski MD, Zhang Y, Long M. General gene movement off the X chromosome in the
847 Drosophila genus. Genome Res. 2009;19(5):897-903. Epub 2009/03/03. doi:
848 10.1101/gr.088609.108. PubMed PMID: 19251740; PubMed Central PMCID: PMCPMC2675978.
849 18. Vibranovski MD, Zhang YE, Kemkemer C, Lopes HF, Karr TL, Long M. Re-analysis of the
850 larval testis data on meiotic sex chromosome inactivation revealed evidence for tissue-specific
851 gene expression related to the drosophila X chromosome. BMC Biology. 2012;10(1):49. doi:
852 10.1186/1741-7007-10-49.
853 19. Landeen EL, Muirhead CA, Wright L, Meiklejohn CD, Presgraves DC. Sex Chromosome-
854 wide Transcriptional Suppression and Compensatory Cis-Regulatory Evolution Mediate Gene
855 Expression in the Drosophila Male Germline. PLOS Biology. 2016;14(7):e1002499. doi:
856 10.1371/journal.pbio.1002499.
857 20. Kemkemer C, Hense W, Parsch J. Fine-Scale Analysis of X Chromosome Inactivation in
858 the Male Germ Line of Drosophila melanogaster. Molecular Biology and Evolution.
859 2011;28(5):1561-3. doi: 10.1093/molbev/msq355.
860 21. Meiklejohn CD, Landeen EL, Cook JM, Kingan SB, Presgraves DC. Sex Chromosome-
861 Specific Regulation in the Drosophila Male Germline But Little Evidence for Chromosomal
862 Dosage Compensation or Meiotic Inactivation. PLoS Biology. 2011;9(8):e1001126. doi:
863 10.1371/journal.pbio.1001126.
864 22. Mikhaylova LM, Nurminsky DI. Lack of global meiotic sex chromosome inactivation, and
865 paucity of tissue-specific gene expression on the Drosophila X chromosome. BMC Biology.
866 2011;9(1):29. doi: 10.1186/1741-7007-9-29.
867 23. Betrán E, Thornton K, Long M. Retroposed new genes out of the X in Drosophila.
868 Genome Res. 2002;12(12):1854-9. Epub 2002/12/06. doi: 10.1101/gr.6049. PubMed PMID:
869 12466289; PubMed Central PMCID: PMCPMC187566.
870 24. Parisi M, Nuttall R, Naiman D, Bouffard G, Malley J, Andrews J, et al. Paucity of genes on
871 the Drosophila X chromosome showing male-biased expression. Science. 2003;299(5607):697-
872 700. Epub 2003/01/04. doi: 10.1126/science.1079190. PubMed PMID: 12511656; PubMed
873 Central PMCID: PMCPMC1363366.
874 25. Wang PJ. X chromosomes, retrogenes and their role in male reproduction. Trends
875 Endocrinol Metab. 2004;15(2):79-83. Epub 2004/03/24. doi: 10.1016/j.tem.2004.01.007.
876 PubMed PMID: 15036254.
877 26. Kruger AN, Brogley MA, Huizinga JL, Kidd JM, De Rooij DG, Hu Y-C, et al. A
878 Neofunctionalized X-Linked Ampliconic Gene Family Is Essential for Male Fertility and Equal Sex
879 Ratio in Mice. Current Biology. 2019;29(21):3699-706.e5. doi: 10.1016/j.cub.2019.08.057.
880 27. Mueller JL, Mahadevaiah SK, Park PJ, Warburton PE, Page DC, Turner JMA. The mouse X
881 chromosome is enriched for multicopy testis genes showing postmeiotic expression. Nature
882 Genetics. 2008;40(6):794-9. doi: 10.1038/ng.126.
883 28. Hughes JF, Skaletsky H, Pyntikova T, Koutseva N, Raudsepp T, Brown LG, et al. Sequence
884 analysis in Bos taurus reveals pervasiveness of X–Y arms races in mammalian lineages. Genome
885 Research. 2020;30(12):1716-26. doi: 10.1101/gr.269902.120.

886 29. Soh YQ, Alföldi J, Pyntikova T, Laura, Graves T, Patrick, et al. Sequencing the Mouse Y
887 Chromosome Reveals Convergent Gene Acquisition and Amplification on Both Sex
888 Chromosomes. Cell. 2014;159(4):800-13. doi: 10.1016/j.cell.2014.09.052.
889 30. Bellott DW, Skaletsky H, Cho T-J, Brown L, Locke D, Chen N, et al. Avian W and
890 mammalian Y chromosomes convergently retained dosage-sensitive regulators. Nature
891 Genetics. 2017;49(3):387-94. doi: 10.1038/ng.3778.
892 31. Guioli S, Lovell-Badge R, Turner JMA. Error-Prone ZW Pairing and No Evidence for
893 Meiotic Sex Chromosome Inactivation in the Chicken Germ Line. PLoS Genetics.
894 2012;8(3):e1002560. doi: 10.1371/journal.pgen.1002560.
895 32. Federici F, Mulugeta E, Schoenmakers S, Wassenaar E, Hoogerbrugge JW, Van Der
896 Heijden GW, et al. Incomplete meiotic sex chromosome inactivation in the domestic dog. BMC
897 Genomics. 2015;16(1). doi: 10.1186/s12864-015-1501-9.
898 33. Darolti I, Wright AE, Mank JE. Guppy Y Chromosome Integrity Maintained by Incomplete
899 Recombination Suppression. Genome Biology and Evolution. 2020;12(6):965-77. doi:
900 10.1093/gbe/evaa099.
901 34. Wright AE, Darolti I, Bloch NI, Oostra V, Sandkam B, Buechel SD, et al. Convergent
902 recombination suppression suggests role of sexual selection in guppy sex chromosome
903 formation. Nature Communications. 2017;8(1):14251. doi: 10.1038/ncomms14251.
904 35. Charlesworth D, Bergero R, Graham C, Gardner J, Keegan K. How did the guppy Y
905 chromosome evolve? PLOS Genetics. 2021;17(8):e1009704. doi:
906 10.1371/journal.pgen.1009704.
907 36. Lisachov AP, Zadesenets KS, Rubtsov NB, Borodin PM. Sex chromosome synapsis and
908 recombination in male guppies. Zebrafish. 2015;12(2):174-80. Epub 2015/01/22. doi:
909 10.1089/zeb.2014.1000. PubMed PMID: 25608108.
910 37. Peichel CL, McCann SR, Ross JA, Naftaly AFS, Urton JR, Cech JN, et al. Assembly of the
911 threespine stickleback Y chromosome reveals convergent signatures of sex chromosome
912 evolution. Genome Biology. 2020;21(1). doi: 10.1186/s13059-020-02097-x.
913 38. Roesti M, Moser D, Berner D. Recombination in the threespine stickleback genome—
914 patterns and consequences. Molecular Ecology. 2013;22(11):3014-27. doi: 10.1111/mec.12322.
915 39. White MA, Kitano J, Peichel CL. Purifying Selection Maintains Dosage-Sensitive Genes
916 during Degeneration of the Threespine Stickleback Y Chromosome. Molecular Biology and
917 Evolution. 2015;32(8):1981-95. doi: 10.1093/molbev/msv078.
918 40. Ross JA, Peichel CL. Molecular cytogenetic evidence of rearrangements on the Y
919 chromosome of the threespine stickleback fish. Genetics. 2008;179(4):2173-82. Epub
920 2008/08/12. doi: 10.1534/genetics.108.088559. PubMed PMID: 18689886; PubMed Central
921 PMCID: PMCPMC2516089.
922 41. Nath S, Welch LA, Flanagan MK, White MA. Meiotic pairing and double-strand break
923 formation along the heteromorphic threespine stickleback sex chromosomes. Chromosome
924 Research. 2022. doi: 10.1007/s10577-022-09699-0.
925 42. Lukassen S, Bosch E, Ekici AB, Winterpacht A. Single-cell RNA sequencing of adult mouse
926 testes. Scientific Data. 2018;5(1):180192. doi: 10.1038/sdata.2018.192.
927 43. Craig-Bennett A. V. The reproductive cycle of the three-spined stickleback,
928 Gasterosteus aculeatus , Linn. Philosophical Transactions of the Royal Society of London

929 Series B, Containing Papers of a Biological Character. 1931;219(462-467):197-279. doi:
930 10.1098/rstb.1931.0005.
931 44. Heumos L, Schaar AC, Lance C, Litinetskaya A, Drost F, Zappia L, et al. Best practices for
932 single-cell analysis across modalities. Nature Reviews Genetics. 2023;24(8):550-72. doi:
933 10.1038/s41576-023-00586-w.
934 45. Witt E, Benjamin S, Svetec N, Zhao L. Testis single-cell RNA-seq reveals the dynamics of
935 de novo gene transcription and germline mutational bias in Drosophila. eLife. 2019;8. doi:
936 10.7554/elife.47138.
937 46. Bonilla E, Xu EY. Identification and characterization of novel mammalian spermatogenic
938 genes conserved from fly to human. Molecular Human Reproduction. 2008;14(3):137-42. doi:
939 10.1093/molehr/gan002.
940 47. Lukassen S, Bosch E, Ekici AB, Winterpacht A. Characterization of germ cell
941 differentiation in the male mouse through single-cell RNA sequencing. Scientific Reports.
942 2018;8(1). doi: 10.1038/s41598-018-24725-0.
943 48. Shami AN, Zheng X, Munyoki SK, Ma Q, Manske GL, Green CD, et al. Single-Cell RNA
944 Sequencing of Human, Macaque, and Mouse Testes Uncovers Conserved and Divergent
945 Features of Mammalian Spermatogenesis. Developmental Cell. 2020;54(4):529-47.e12. doi:
946 10.1016/j.devcel.2020.05.010.
947 49. Green CD, Ma Q, Manske GL, Shami AN, Zheng X, Marini S, et al. A Comprehensive
948 Roadmap of Murine Spermatogenesis Defined by Single-Cell RNA-Seq. Developmental Cell.
949 2018;46(5):651-67.e10. doi: 10.1016/j.devcel.2018.07.025.
950 50. Hermann BP, Cheng K, Singh A, Roa-De La Cruz L, Mutoji KN, Chen IC, et al. The
951 Mammalian Spermatogenesis Single-Cell Transcriptome, from Spermatogonial Stem Cells to
952 Spermatids. Cell Reports. 2018;25(6):1650-67.e8. doi: 10.1016/j.celrep.2018.10.026.
953 51. Qian P, Kang J, Liu D, Xie G. Single Cell Transcriptome Sequencing of Zebrafish Testis
954 Revealed Novel Spermatogenesis Marker Genes and Stronger Leydig-Germ Cell Paracrine
955 Interactions. Frontiers in Genetics. 2022;13.
956 52. Wu X, Yang Y, Zhong C, Wang T, Deng Y, Huang H, et al. Single-Cell Atlas of Adult Testis
957 in Protogynous Hermaphroditic Orange-Spotted Grouper, Epinephelus coioides. International
958 Journal of Molecular Sciences. 2021;22(22):12607. doi: 10.3390/ijms222212607.
959 53. Lacerda SMdSN, Costa GMJ, de França LR. Biology and identity of fish spermatogonial
960 stem cell. General and Comparative Endocrinology. 2014;207:56-65. doi:
961 https://doi.org/10.1016/j.ygcen.2014.06.018.
962 54. Xie X, Nóbrega R, Pšenička M. Spermatogonial Stem Cells in Fish: Characterization,
963 Isolation, Enrichment, and Recent Advances of In Vitro Culture Systems. Biomolecules.
964 2020;10(4):644. doi: 10.3390/biom10040644.
965 55. Jin C, Yan K, Wang M, Song W, Wang B, Men Y, et al. Dissecting the dynamic cellular
966 transcriptional atlas of adult teleost testis development throughout the annual reproductive
967 cycle. Development. 2024;151(20). doi: 10.1242/dev.202296.
968 56. Fuess LE, Bolnick DI. Single-Cell RNA Sequencing Reveals Microevolution of the
969 Stickleback Immune System. Genome Biology and Evolution. 2023;15(4). doi:
970 10.1093/gbe/evad053.

971 57. Hirota T, Blakeley P, Sangrithi MN, Mahadevaiah SK, Encheva V, Snijders AP, et al.
972 SETDB1 Links the Meiotic DNA Damage Response to Sex Chromosome Silencing in Mice.
973 Developmental Cell. 2018;47(5):645-59.e6. doi: 10.1016/j.devcel.2018.10.004.
974 58. Sedelnikova OA, Pilch DR, Redon C, Bonner WM. Histone H2AX in DNA damage and
975 repair. Cancer Biol Ther. 2003;2(3):233-5. Epub 2003/07/25. doi: 10.4161/cbt.2.3.373. PubMed
976 PMID: 12878854.
977 59. Shaw DE, White MA. The evolution of gene regulation on sex chromosomes. Trends in
978 Genetics. 2022. doi: 10.1016/j.tig.2022.04.004.
979 60. Beaudry FEG, Barrett SCH, Wright SI. Genomic Loss and Silencing on the Y Chromosomes
980 of Rumex. Genome Biology and Evolution. 2017;9(12):3345-55. doi: 10.1093/gbe/evx254.
981 61. Veltsos P, Ridout KE, Toups MA, González-Martínez SC, Muyle A, Emery O, et al. Early
982 Sex-Chromosome Evolution in the Diploid Dioecious Plant Mercurialis annua. Genetics.
983 2019;212(3):815-35. doi: 10.1534/genetics.119.302045.
984 62. Wei KHC, Bachtrog D. Ancestral male recombination in Drosophila albomicans produced
985 geographically restricted neo-Y chromosome haplotypes varying in age and onset of decay.
986 PLOS Genetics. 2019;15(11):e1008502. doi: 10.1371/journal.pgen.1008502.
987 63. Martin H, Carpentier F, Gallina S, Godé C, Schmitt E, Muyle A, et al. Evolution of Young
988 Sex Chromosomes in Two Dioecious Sister Plant Species with Distinct Sex Determination
989 Systems. Genome Biology and Evolution. 2019;11(2):350-61. doi: 10.1093/gbe/evz001.
990 64. Koslowski M, Sahin U, Huber C, Türeci O. The human X chromosome is enriched for
991 germline genes expressed in premeiotic germ cells of both sexes. Hum Mol Genet.
992 2006;15(15):2392-9. Epub 2006/07/01. doi: 10.1093/hmg/ddl163. PubMed PMID: 16809397.
993 65. Shaw DE, Naftaly AS, White MA. Positive Selection Drives cis-regulatory Evolution Across
994 the Threespine Stickleback Y Chromosome. Molecular Biology and Evolution. 2024;41(2). doi:
995 10.1093/molbev/msae020.
996 66. Martínez-Pacheco M, Tenorio M, Almonte L, Fajardo V, Godínez A, Fernández D, et al.
997 Expression Evolution of Ancestral XY Gametologs across All Major Groups of Placental
998 Mammals. Genome Biology and Evolution. 2020;12(11):2015-28. doi: 10.1093/gbe/evaa173.
999 67. Bachtrog D. Y-chromosome evolution: emerging insights into processes of Y-
1000 chromosome degeneration. Nature Reviews Genetics. 2013;14(2):113-24. doi:
1001 10.1038/nrg3366.
1002 68. Cocquet J, Ellis PJI, Mahadevaiah SK, Affara NA, Vaiman D, Burgoyne PS. A Genetic Basis
1003 for a Postmeiotic X Versus Y Chromosome Intragenomic Conflict in the Mouse. PLoS Genetics.
1004 2012;8(9):e1002900. doi: 10.1371/journal.pgen.1002900.
1005 69. Cocquet J, Ellis PJI, Yamauchi Y, Mahadevaiah SK, Affara NA, Ward MA, et al. The
1006 Multicopy Gene Sly Represses the Sex Chromosomes in the Male Mouse Germline after
1007 Meiosis. PLoS Biology. 2009;7(11):e1000244. doi: 10.1371/journal.pbio.1000244.
1008 70. Bachtrog D, Mahajan S, Bracewell R. Massive gene amplification on a recently formed
1009 Drosophila Y chromosome. Nature Ecology & Evolution. 2019;3(11):1587-97. doi:
1010 10.1038/s41559-019-1009-9.
1011 71. Hirano T. At the heart of the chromosome: SMC proteins in action. Nature Reviews
1012 Molecular Cell Biology. 2006;7(5):311-22. doi: 10.1038/nrm1909.

72. Moretti C, Vaiman D, Tores F, Cocquet J. Expression and epigenomic landscape of the sex chromosomes in mouse post-meiotic male germ cells. Epigenetics & Chromatin. 2016;9(1). doi: 10.1186/s13072-016-0099-8.
73. Emerson JJ, Kaessmann H, Betrán E, Long M. Extensive Gene Traffic on the Mammalian X Chromosome. Science. 2004;303(5657):537-40. doi: doi:10.1126/science.1090042.
74. Shiao M-S, Khil P, Camerini-Otero RD, Shiroishi T, Moriwaki K, Yu H-T, et al. Origins of New Male Germ-line Functions from X-Derived Autosomal Retrogenes in the Mouse. Molecular Biology and Evolution. 2007;24(10):2242-53. doi: 10.1093/molbev/msm153.
75. Bell MA, Stewart JD, Park PJ. The World's Oldest Fossil Threespine Stickleback Fish. Copeia. 2009;2009(2):256-65. doi: 10.1643/cg-08-059.
76. Ross JA, Urton JR, Boland J, Shapiro MD, Peichel CL. Turnover of Sex Chromosomes in the Stickleback Fishes (Gasterosteidae). PLoS Genetics. 2009;5(2):e1000391. doi: 10.1371/journal.pgen.1000391.
77. Varadharajan S, Rastas P, Löytynoja A, Matschiner M, Calboli FCF, Guo B, et al. A high-quality assembly of the nine-spined stickleback (Pungitius pungitius) genome. Genome Biology and Evolution. 2019. doi: 10.1093/gbe/evz240.
78. Graves JAM. Evolution of vertebrate sex chromosomes and dosage compensation. Nature Reviews Genetics. 2016;17(1):33-46. doi: 10.1038/nrg.2015.2.
79. Mank JE, Ellegren H. All dosage compensation is local: Gene-by-gene regulation of sex-biased expression on the chicken Z chromosome. Heredity. 2009;102(3):312-20. doi: 10.1038/hdy.2008.116.
80. Mullon C, Wright AE, Reuter M, Pomiankowski A, Mank JE. Evolution of dosage compensation under sexual selection differs between X and Z chromosomes. Nature Communications. 2015;6(1):7720. doi: 10.1038/ncomms8720.
81. Wei KHC, Chatla K, Bachtrog D. Single-cell RNA-seq of Drosophila miranda testis reveals the evolution and trajectory of germline sex chromosome regulation. PLOS Biology. 2024;22(4):e3002605. doi: 10.1371/journal.pbio.3002605.
82. Witt E, Shao Z, Hu C, Krause HM, Zhao L. Single-cell RNA-sequencing reveals pre-meiotic X-chromosome dosage compensation in Drosophila testis. PLOS Genetics. 2021;17(8):e1009728. doi: 10.1371/journal.pgen.1009728.
83. Mrnjavac A, Khudiakova KA, Barton NH, Vicoso B. Slower-X: reduced efficiency of selection in the early stages of X chromosome evolution. Evolution Letters. 2023;7(1):4-12. doi: 10.1093/evlett/qrac004.
84. Good JM, Nachman MW. Rates of protein evolution are positively correlated with developmental timing of expression during mouse spermatogenesis. Mol Biol Evol. 2005;22(4):1044-52. Epub 2005/01/14. doi: 10.1093/molbev/msi087. PubMed PMID: 15647515.
85. Kopania EEK, Larson EL, Callahan C, Keeble S, Good JM. Molecular Evolution across Mouse Spermatogenesis. Molecular Biology and Evolution. 2022;39(2). doi: 10.1093/molbev/msac023.
86. Larson EL, Vanderpool D, Keeble S, Zhou M, Sarver BA, Smith AD, et al. Contrasting Levels of Molecular Evolution on the Mouse X Chromosome. Genetics. 2016;203(4):1841-57. Epub 2016/06/19. doi: 10.1534/genetics.116.186825. PubMed PMID: 27317678; PubMed Central PMCID: PMCPMC4981281.

1057 87. Lifschytz E, Lindsley DL. The role of X-chromosome inactivation during spermatogenesis.
1058 Proceedings of the National Academy of Sciences. 1972;69(1):182-6.
1059 88. McKee BD, Handel MA. Sex chromosomes, recombination, and chromatin conformation.
1060 Chromosoma. 1993;102(2):71-80. doi: 10.1007/BF00356023.
1061 89. Solari AJ. Equalization of Z and W axes in chicken and quail oocytes. Cytogenet Cell
1062 Genet. 1992;59(1):52-6. Epub 1992/01/01. doi: 10.1159/000133199. PubMed PMID: 1733674.
1063 90. Meiklejohn CD, Tao Y. Genetic conflict and sex chromosome evolution. Trends in
1064 Ecology & Evolution. 2010;25(4):215-23. doi: 10.1016/j.tree.2009.10.005.
1065 91. Wu C-I, Yujun Xu E. Sexual antagonism and X inactivation – the SAXI hypothesis. Trends
1066 in Genetics. 2003;19(5):243-7. doi: 10.1016/s0168-9525(03)00058-1.
1067 92. Good JM. The Conflict within and the Escalating War between the Sex Chromosomes.
1068 PLoS Genetics. 2012;8(9):e1002955. doi: 10.1371/journal.pgen.1002955.
1069 93. Casey AE, Daish TJ, Barbero JL, Grützner F. Differential cohesin loading marks paired and
1070 unpaired regions of platypus sex chromosomes at prophase I. Scientific Reports.
1071 2017;7(1):4217. doi: 10.1038/s41598-017-04560-5.
1072 94. Schoenmakers S, Wassenaar E, Hoogerbrugge JW, Laven JSE, Grootegoed JA, Baarends
1073 WM. Female Meiotic Sex Chromosome Inactivation in Chicken. PLoS Genetics.
1074 2009;5(5):e1000466. doi: 10.1371/journal.pgen.1000466.
1075 95. Namekawa SH, Lee JT. XY and ZW: is meiotic sex chromosome inactivation the rule in
1076 evolution? PLoS Genet. 2009;5(5):e1000493. Epub 2009/05/23. doi:
1077 10.1371/journal.pgen.1000493. PubMed PMID: 19461890; PubMed Central PMCID:
1078 PMCPMC2679206.
1079 96. Vibranovski MD, Lopes HF, Karr TL, Long M. Stage-Specific Expression Profiling of
1080 Drosophila Spermatogenesis Suggests that Meiotic Sex Chromosome Inactivation Drives
1081 Genomic Relocation of Testis-Expressed Genes. PLoS Genetics. 2009;5(11):e1000731. doi:
1082 10.1371/journal.pgen.1000731.
1083 97. Mahadevaraju S, Fear JM, Akeju M, Galletta BJ, Pinheiro MMLS, Avelino CC, et al.
1084 Dynamic sex chromosome expression in Drosophila male germ cells. Nature Communications.
1085 2021;12(1). doi: 10.1038/s41467-021-20897-y.
1086 98. Vibranovski MD. Meiotic sex chromosome inactivation in Drosophila. J Genomics.
1087 2014;2:104-17. Epub 2014/07/25. doi: 10.7150/jgen.8178. PubMed PMID: 25057326; PubMed
1088 Central PMCID: PMCPMC4105432.
1089 99. Viera A, Parra MT, Arévalo S, García De La Vega C, Santos JL, Page J. X Chromosome
1090 Inactivation during Grasshopper Spermatogenesis. Genes. 2021;12(12):1844. doi:
1091 10.3390/genes12121844.
1092 100. Page N, Taxiarchi C, Tonge D, Kuburic J, Chesters E, Kriezis A, et al. Single-cell profiling of
1093 Anopheles gambiae spermatogenesis defines the onset of meiotic silencing and premeiotic
1094 overexpression of the X chromosome. Communications Biology. 2023;6(1):850. doi:
1095 10.1038/s42003-023-05224-z.
1096 101. Taxiarchi C, Kranjc N, Kriezis A, Kyrou K, Bernardini F, Russell S, et al. High-resolution
1097 transcriptional profiling of Anopheles gambiae spermatogenesis reveals mechanisms of sex
1098 chromosome regulation. Scientific Reports. 2019;9(1). doi: 10.1038/s41598-019-51181-1.
1099 102. Lisachov A, Dedukh D, Simanovsky S, Panthum T, Singchat W, Srikulnath K. Spaghetti
1100 Connections: Synaptonemal Complexes as a Tool to Explore Chromosome Structure, Evolution,

and Meiotic Behavior in Fish. Cytogenet Genome Res. 2024;164(1):1-15. Epub 2024/03/08. doi: 10.1159/000538238. PubMed PMID: 38452741.
103. Nanda I, Schories S, Simeonov I, Adolfi MC, Du K, Steinlein C, et al. Evolution of the Degenerated Y-Chromosome of the Swamp Guppy, Micropoecilia picta. Cells. 2022;11(7). Epub 2022/04/13. doi: 10.3390/cells11071118. PubMed PMID: 35406682; PubMed Central PMCID: PMCPMC8997885.
104. Bachtrog D. The Y Chromosome as a Battleground for Intragenomic Conflict. Trends Genet. 2020;36(7):510-22. Epub 2020/05/26. doi: 10.1016/j.tig.2020.04.008. PubMed PMID: 32448494; PubMed Central PMCID: PMCPMC8329999.
105. Mank JE, Hosken DJ, Wedell N. Conflict on the sex chromosomes: cause, effect, and complexity. Cold Spring Harb Perspect Biol. 2014;6(12):a017715. Epub 2014/10/05. doi: 10.1101/cshperspect.a017715. PubMed PMID: 25280765; PubMed Central PMCID: PMCPMC4292157.
106. Chang C-H, Gregory LE, Gordon KE, Meiklejohn CD, Larracuente AM. Unique structure and positive selection promote the rapid divergence of Drosophila Y chromosomes. eLife. 2022;11. doi: 10.7554/elife.75795.
107. Lin Y, Darolti I, Furman BLS, Almeida P, Sandkam BA, Breden F, et al. Gene duplication to the Y chromosome in Trinidadian Guppies. Molecular Ecology. 2022;31(6):1853-63. doi: 10.1111/mec.16355.
108. Moretti C, Blanco M, Ialy-Radio C, Serrentino ME, Gobé C, Friedman R, et al. Battle of the Sex Chromosomes: Competition between X and Y Chromosome-Encoded Proteins for Partner Interaction and Chromatin Occupancy Drives Multicopy Gene Expression and Evolution in Muroid Rodents. Mol Biol Evol. 2020;37(12):3453-68. Epub 2020/07/14. doi: 10.1093/molbev/msaa175. PubMed PMID: 32658962; PubMed Central PMCID: PMCPMC7743899.
109. Mueller JL, Skaletsky H, Brown LG, Zaghlul S, Rock S, Graves T, et al. Independent specialization of the human and mouse X chromosomes for the male germ line. Nature Genetics. 2013;45(9):1083-7. doi: 10.1038/ng.2705.
110. Liu J, Shikano T, Leinonen T, Cano JM, Li M-H, Merilä J. Identification of Major and Minor QTL for Ecologically Important Morphological Traits in Three-Spined Sticklebacks (Gasterosteus aculeatus). G3 Genes|Genomes|Genetics. 2014;4(4):595-604. doi: 10.1534/g3.114.010389.
111. Rollins JL, Chiang P, Waite JN, Von Hippel FA, Bell MA. Jacks and jills: Alternative life-history phenotypes and skewed sex ratio in anadromous threespine stickleback (Gasterosteus aculeatus). Evolutionary Ecology Research. 2017;18(4):363-82.
112. Chang C-H, Mejia Natividad I, Malik HS. Expansion and loss of sperm nuclear basic protein genes in Drosophila correspond with genetic conflicts between sex chromosomes. eLife. 2023;12:e85249. doi: 10.7554/eLife.85249.
113. Larracuente AM, Presgraves DC. The SelfishSegregation DistorterGene Complex ofDrosophila melanogaster. Genetics. 2012;192(1):33-53. doi: 10.1534/genetics.112.141390.
114. Ellis PJI, Bacon J, Affara NA. Association of Sly with sex-linked gene amplification during mouse evolution: a side effect of genomic conflict in spermatids? Human Molecular Genetics. 2011;20(15):3010-21. doi: 10.1093/hmg/ddr204.

115. Olds-Clarke P. Models for male infertility: the t haplotypes. Rev Reprod. 1997;2(3):157-64. Epub 1998/01/01. doi: 10.1530/ror.0.0020157. PubMed PMID: 9414479.
116. Phadnis N, Orr HA. A Single Gene Causes Both Male Sterility and Segregation Distortion in Drosophila Hybrids. Science. 2009;323(5912):376-9. doi: 10.1126/science.1163934.
117. Fitzpatrick JL. Sperm competition and fertilization mode in fishes. Philosophical Transactions of the Royal Society B: Biological Sciences. 2020;375(1813):20200074. doi: 10.1098/rstb.2020.0074.
118. Verspoor RL, Price TAR, Wedell N. Selfish genetic elements and male fertility. Philos Trans R Soc Lond B Biol Sci. 2020;375(1813):20200067. Epub 2020/10/20. doi: 10.1098/rstb.2020.0067. PubMed PMID: 33070738; PubMed Central PMCID: PMCPMC7661447.
119. Van den Assem J. Territory in the three-spined stickleback Gasterosteus aculeatus L.: an experimental study in intra-specific competition: Brill Archive; 1967.
120. Largiadèr CR, Fries V, Bakker TCM. Genetic analysis of sneaking and egg-thievery in a natural population of the three-spined stickleback (Gasterosteus aculeatus L.). Heredity. 2001;86(4):459-68. doi: 10.1046/j.1365-2540.2001.00850.x.
121. Nath S, Shaw DE, White MA. Improved contiguity of the threespine stickleback genome using long-read sequencing. G3 Genes|Genomes|Genetics. 2021;11(2). doi: 10.1093/g3journal/jkab007.
122. Hao Y, Hao S, Andersen-Nissen E, Mauck WM, Zheng S, Butler A, et al. Integrated analysis of multimodal single-cell data. Cell. 2021;184(13):3573-87.e29. doi: 10.1016/j.cell.2021.04.048.
123. Sokołowska E, Kulczykowska E. Annual reproductive cycle in two free living populations of three-spined stickleback (Gasterosteus aculeatus L.): Patterns of ovarian and testicular development. Oceanologia. 2006;48.
124. Borg B. Effects of methyltestosterone on spermatogenesis and secondary sexual characters in the three-spined stickleback (Gasterosteus aculeatus L.). General and Comparative Endocrinology. 1981;44(2):177-80. doi: 10.1016/0016-6480(81)90245-8.
125. Dapper AL, Payseur BA. Molecular evolution of the meiotic recombination pathway in mammals. Evolution. 2019;73(12):2368-89. doi: 10.1111/evo.13850.
126. Ramesh MA, Malik S-B, Logsdon JM. A Phylogenomic Inventory of Meiotic Genes. Current Biology. 2005;15(2):185-91. doi: 10.1016/j.cub.2005.01.003.
127. Anders S, Pyl PT, Huber W. HTSeq--a Python framework to work with high-throughput sequencing data. Bioinformatics. 2015;31(2):166-9. doi: 10.1093/bioinformatics/btu638.
128. Wang D, Rastas P, Yi X, Löytynoja A, Kivikoski M, Feng X, et al. Improved assembly of the Pungitius pungitius reference genome. G3 Genes|Genomes|Genetics. 2024;14(8). doi: 10.1093/g3journal/jkae126.
129. Slater GSC, Birney E. Automated generation of heuristics for biological sequence comparison. BMC Bioinformatics. 2005;6(1):31. doi: 10.1186/1471-2105-6-31.
130. Cunningham F, Allen JE, Allen J, Alvarez-Jarreta J, Amode M R, Armean Irina M, et al. Ensembl 2022. Nucleic Acids Research. 2021;50(D1):D988-D95. doi: 10.1093/nar/gkab1049.
131. Yang Z. PAML 4: Phylogenetic Analysis by Maximum Likelihood. Molecular Biology and Evolution. 2007;24(8):1586-91. doi: 10.1093/molbev/msm088.
132. Blokhina YP, Nguyen AD, Draper BW, Burgess SM. The telomere bouquet is a hub where meiotic double-strand breaks, synapsis, and stable homolog juxtaposition are coordinated in

the zebrafish, Danio rerio. PLoS Genet. 2019;15(1):e1007730. Epub 2019/01/18. doi: 10.1371/journal.pgen.1007730. PubMed PMID: 30653507; PubMed Central PMCID: PMCPMC6336226.

1. Ellis N, Goodfellow PN. The mammalian pseudoautosomal region. Trends in Genetics. 1989;5:406-10. doi: https://doi.org/10.1016/0168-9525(89)90199-6.
2. Turner JMA. Meiotic sex chromosome inactivation. Development. 2007;134(10):1823-31. doi: 10.1242/dev.000018.
3. Turner JMA. Meiotic Silencing in Mammals. Annual Review of Genetics. 2015;49(1):395-412. doi: 10.1146/annurev-genet-112414-055145.
4. Handel MA. The XY body: a specialized meiotic chromatin domain. Exp Cell Res. 2004;296(1):57-63. Epub 2004/05/04. doi: 10.1016/j.yexcr.2004.03.008. PubMed PMID: 15120994.
5. Namekawa SH, Park PJ, Zhang L-F, Shima JE, McCarrey JR, Griswold MD, et al. Postmeiotic Sex Chromatin in the Male Germline of Mice. Current Biology. 2006;16(7):660-7. doi: 10.1016/j.cub.2006.01.066.
6. Turner JMA, Mahadevaiah SK, Ellis PJI, Mitchell MJ, Burgoyne PS. Pachytene Asynapsis Drives Meiotic Sex Chromosome Inactivation and Leads to Substantial Postmeiotic Repression in Spermatids. Developmental Cell. 2006;10(4):521-9. doi: 10.1016/j.devcel.2006.02.009.
7. Shiu PK, Raju NB, Zickler D, Metzenberg RL. Meiotic silencing by unpaired DNA. Cell. 2001;107(7):905-16. Epub 2002/01/10. doi: 10.1016/s0092-8674(01)00609-2. PubMed PMID: 11779466.
8. Turner JM, Mahadevaiah SK, Fernandez-Capetillo O, Nussenzweig A, Xu X, Deng CX, et al. Silencing of unsynapsed meiotic chromosomes in the mouse. Nat Genet. 2005;37(1):41-7. Epub 2004/12/08. doi: 10.1038/ng1484. PubMed PMID: 15580272.
9. Cortez D, Marin R, Toledo-Flores D, Froidevaux L, Liechti A, Waters PD, et al. Origins and functional evolution of Y chromosomes across mammals. Nature. 2014;508(7497):488-93. doi: 10.1038/nature13151.
10. Franco MJ, Sciurano RB, Solari AJ. Protein immunolocalization supports the presence of identical mechanisms of XY body formation in eutherians and marsupials. Chromosome Research. 2007;15(6):815-24. doi: 10.1007/s10577-007-1165-7.
11. Namekawa SH, Vandeberg JL, McCarrey JR, Lee JT. Sex chromosome silencing in the marsupial male germ line. Proceedings of the National Academy of Sciences. 2007;104(23):9730-5. doi: 10.1073/pnas.0700323104.
12. Daish TJ, Casey AE, Grutzner F. Lack of sex chromosome specific meiotic silencing in platypus reveals origin of MSCI in therian mammals. BMC Biology. 2015;13(1). doi: 10.1186/s12915-015-0215-4.
13. Murat F, Mbengue N, Winge SB, Trefzer T, Leushkin E, Sepp M, et al. The molecular evolution of spermatogenesis across mammals. Nature. 2023;613(7943):308-16. doi: 10.1038/s41586-022-05547-7.

1229 14. Larson BJ, Van MV, Nakayama T, Engebrecht J. Plasticity in the Meiotic Epigenetic
1230 Landscape of Sex Chromosomes in Caenorhabditis Species. Genetics. 2016;203(4):1641-
1231 58. doi: 10.1534/genetics.116.191130.
1232 15. Cabrero J, Teruel M, Carmona FD, Camacho JP. Histone H2AX phosphorylation is
1233 associated with most meiotic events in grasshopper. Cytogenet Genome Res. 2007;116(4):311-
1234 5. Epub 2007/04/14. doi: 10.1159/000100416. PubMed PMID: 17431330.
1235 16. Cabrero J, Teruel M, Carmona FD, Jiménez R, Camacho JP. Histone H3 lysine 9
1236 acetylation pattern suggests that X and B chromosomes are silenced during entire male meiosis
1237 in a grasshopper. Cytogenet Genome Res. 2007;119(1-2):135-42. Epub 2007/12/28. doi:
1238 10.1159/000109630. PubMed PMID: 18160793.
1239 17. Vibranovski MD, Zhang Y, Long M. General gene movement off the X chromosome in the
1240 Drosophila genus. Genome Res. 2009;19(5):897-903. Epub 2009/03/03. doi:
1241 10.1101/gr.088609.108. PubMed PMID: 19251740; PubMed Central PMCID: PMCPMC2675978.
1242 18. Vibranovski MD, Zhang YE, Kemkemer C, Lopes HF, Karr TL, Long M. Re-analysis of the
1243 larval testis data on meiotic sex chromosome inactivation revealed evidence for tissue-specific
1244 gene expression related to the drosophila X chromosome. BMC Biology. 2012;10(1):49. doi:
1245 10.1186/1741-7007-10-49.
1246 19. Landeen EL, Muirhead CA, Wright L, Meiklejohn CD, Presgraves DC. Sex Chromosome-
1247 wide Transcriptional Suppression and Compensatory Cis-Regulatory Evolution Mediate Gene
1248 Expression in the Drosophila Male Germline. PLOS Biology. 2016;14(7):e1002499. doi:
1249 10.1371/journal.pbio.1002499.
1250 20. Kemkemer C, Hense W, Parsch J. Fine-Scale Analysis of X Chromosome Inactivation in
1251 the Male Germ Line of Drosophila melanogaster. Molecular Biology and Evolution.
1252 2011;28(5):1561-3. doi: 10.1093/molbev/msq355.
1253 21. Meiklejohn CD, Landeen EL, Cook JM, Kingan SB, Presgraves DC. Sex Chromosome-
1254 Specific Regulation in the Drosophila Male Germline But Little Evidence for Chromosomal
1255 Dosage Compensation or Meiotic Inactivation. PLoS Biology. 2011;9(8):e1001126. doi:
1256 10.1371/journal.pbio.1001126.
1257 22. Mikhaylova LM, Nurminsky DI. Lack of global meiotic sex chromosome inactivation, and
1258 paucity of tissue-specific gene expression on the Drosophila X chromosome. BMC Biology.
1259 2011;9(1):29. doi: 10.1186/1741-7007-9-29.
1260 23. Betrán E, Thornton K, Long M. Retroposed new genes out of the X in Drosophila.
1261 Genome Res. 2002;12(12):1854-9. Epub 2002/12/06. doi: 10.1101/gr.6049. PubMed PMID:
1262 12466289; PubMed Central PMCID: PMCPMC187566.
1263 24. Parisi M, Nuttall R, Naiman D, Bouffard G, Malley J, Andrews J, et al. Paucity of genes on
1264 the Drosophila X chromosome showing male-biased expression. Science. 2003;299(5607):697-
1265 700. Epub 2003/01/04. doi: 10.1126/science.1079190. PubMed PMID: 12511656; PubMed
1266 Central PMCID: PMCPMC1363366.
1267 25. Wang PJ. X chromosomes, retrogenes and their role in male reproduction. Trends
1268 Endocrinol Metab. 2004;15(2):79-83. Epub 2004/03/24. doi: 10.1016/j.tem.2004.01.007.
1269 PubMed PMID: 15036254.
1270 26. Kruger AN, Brogley MA, Huizinga JL, Kidd JM, De Rooij DG, Hu Y-C, et al. A
1271 Neofunctionalized X-Linked Ampliconic Gene Family Is Essential for Male Fertility and Equal Sex
1272 Ratio in Mice. Current Biology. 2019;29(21):3699-706.e5. doi: 10.1016/j.cub.2019.08.057.

1273 27. Mueller JL, Mahadevaiah SK, Park PJ, Warburton PE, Page DC, Turner JMA. The mouse X
1274 chromosome is enriched for multicopy testis genes showing postmeiotic expression. Nature
1275 Genetics. 2008;40(6):794-9. doi: 10.1038/ng.126.
1276 28. Hughes JF, Skaletsky H, Pyntikova T, Koutseva N, Raudsepp T, Brown LG, et al. Sequence
1277 analysis in Bos taurus reveals pervasiveness of X–Y arms races in mammalian lineages. Genome
1278 Research. 2020;30(12):1716-26. doi: 10.1101/gr.269902.120.
1279 29. Soh YQ, Alföldi J, Pyntikova T, Laura, Graves T, Patrick, et al. Sequencing the Mouse Y
1280 Chromosome Reveals Convergent Gene Acquisition and Amplification on Both Sex
1281 Chromosomes. Cell. 2014;159(4):800-13. doi: 10.1016/j.cell.2014.09.052.
1282 30. Bellott DW, Skaletsky H, Cho T-J, Brown L, Locke D, Chen N, et al. Avian W and
1283 mammalian Y chromosomes convergently retained dosage-sensitive regulators. Nature
1284 Genetics. 2017;49(3):387-94. doi: 10.1038/ng.3778.
1285 31. Guioli S, Lovell-Badge R, Turner JMA. Error-Prone ZW Pairing and No Evidence for
1286 Meiotic Sex Chromosome Inactivation in the Chicken Germ Line. PLoS Genetics.
1287 2012;8(3):e1002560. doi: 10.1371/journal.pgen.1002560.
1288 32. Federici F, Mulugeta E, Schoenmakers S, Wassenaar E, Hoogerbrugge JW, Van Der
1289 Heijden GW, et al. Incomplete meiotic sex chromosome inactivation in the domestic dog. BMC
1290 Genomics. 2015;16(1). doi: 10.1186/s12864-015-1501-9.
1291 33. Darolti I, Wright AE, Mank JE. Guppy Y Chromosome Integrity Maintained by Incomplete
1292 Recombination Suppression. Genome Biology and Evolution. 2020;12(6):965-77. doi:
1293 10.1093/gbe/evaa099.
1294 34. Wright AE, Darolti I, Bloch NI, Oostra V, Sandkam B, Buechel SD, et al. Convergent
1295 recombination suppression suggests role of sexual selection in guppy sex chromosome
1296 formation. Nature Communications. 2017;8(1):14251. doi: 10.1038/ncomms14251.
1297 35. Charlesworth D, Bergero R, Graham C, Gardner J, Keegan K. How did the guppy Y
1298 chromosome evolve? PLOS Genetics. 2021;17(8):e1009704. doi:
1299 10.1371/journal.pgen.1009704.
1300 36. Lisachov AP, Zadesenets KS, Rubtsov NB, Borodin PM. Sex chromosome synapsis and
1301 recombination in male guppies. Zebrafish. 2015;12(2):174-80. Epub 2015/01/22. doi:
1302 10.1089/zeb.2014.1000. PubMed PMID: 25608108.
1303 37. Peichel CL, McCann SR, Ross JA, Naftaly AFS, Urton JR, Cech JN, et al. Assembly of the
1304 threespine stickleback Y chromosome reveals convergent signatures of sex chromosome
1305 evolution. Genome Biology. 2020;21(1). doi: 10.1186/s13059-020-02097-x.
1306 38. Roesti M, Moser D, Berner D. Recombination in the threespine stickleback genome—
1307 patterns and consequences. Molecular Ecology. 2013;22(11):3014-27. doi: 10.1111/mec.12322.
1308 39. White MA, Kitano J, Peichel CL. Purifying Selection Maintains Dosage-Sensitive Genes
1309 during Degeneration of the Threespine Stickleback Y Chromosome. Molecular Biology and
1310 Evolution. 2015;32(8):1981-95. doi: 10.1093/molbev/msv078.
1311 40. Ross JA, Peichel CL. Molecular cytogenetic evidence of rearrangements on the Y
1312 chromosome of the threespine stickleback fish. Genetics. 2008;179(4):2173-82. Epub
1313 2008/08/12. doi: 10.1534/genetics.108.088559. PubMed PMID: 18689886; PubMed Central
1314 PMCID: PMCPMC2516089.

41. Nath S, Welch LA, Flanagan MK, White MA. Meiotic pairing and double-strand break formation along the heteromorphic threespine stickleback sex chromosomes. Chromosome Research. 2022. doi: 10.1007/s10577-022-09699-0.

42. Lukassen S, Bosch E, Ekici AB, Winterpacht A. Single-cell RNA sequencing of adult mouse testes. Scientific Data. 2018;5(1):180192. doi: 10.1038/sdata.2018.192.

43. Craig-Bennett A. V. The reproductive cycle of the three-spined stickleback, Gasterosteus aculeatus , Linn. Philosophical Transactions of the Royal Society of London Series B, Containing Papers of a Biological Character. 1931;219(462-467):197-279. doi: 10.1098/rstb.1931.0005.

44. Heumos L, Schaar AC, Lance C, Litinetskaya A, Drost F, Zappia L, et al. Best practices for single-cell analysis across modalities. Nature Reviews Genetics. 2023;24(8):550-72. doi: 10.1038/s41576-023-00586-w.

45. Witt E, Benjamin S, Svetec N, Zhao L. Testis single-cell RNA-seq reveals the dynamics of de novo gene transcription and germline mutational bias in Drosophila. eLife. 2019;8. doi: 10.7554/elife.47138.

46. Bonilla E, Xu EY. Identification and characterization of novel mammalian spermatogenic genes conserved from fly to human. Molecular Human Reproduction. 2008;14(3):137-42. doi: 10.1093/molehr/gan002.

47. Lukassen S, Bosch E, Ekici AB, Winterpacht A. Characterization of germ cell differentiation in the male mouse through single-cell RNA sequencing. Scientific Reports. 2018;8(1). doi: 10.1038/s41598-018-24725-0.

48. Shami AN, Zheng X, Munyoki SK, Ma Q, Manske GL, Green CD, et al. Single-Cell RNA Sequencing of Human, Macaque, and Mouse Testes Uncovers Conserved and Divergent Features of Mammalian Spermatogenesis. Developmental Cell. 2020;54(4):529-47.e12. doi: 10.1016/j.devcel.2020.05.010.

49. Green CD, Ma Q, Manske GL, Shami AN, Zheng X, Marini S, et al. A Comprehensive Roadmap of Murine Spermatogenesis Defined by Single-Cell RNA-Seq. Developmental Cell. 2018;46(5):651-67.e10. doi: 10.1016/j.devcel.2018.07.025.

50. Hermann BP, Cheng K, Singh A, Roa-De La Cruz L, Mutoji KN, Chen IC, et al. The Mammalian Spermatogenesis Single-Cell Transcriptome, from Spermatogonial Stem Cells to Spermatids. Cell Reports. 2018;25(6):1650-67.e8. doi: 10.1016/j.celrep.2018.10.026.

51. Qian P, Kang J, Liu D, Xie G. Single Cell Transcriptome Sequencing of Zebrafish Testis Revealed Novel Spermatogenesis Marker Genes and Stronger Leydig-Germ Cell Paracrine Interactions. Frontiers in Genetics. 2022;13.

52. Wu X, Yang Y, Zhong C, Wang T, Deng Y, Huang H, et al. Single-Cell Atlas of Adult Testis in Protogynous Hermaphroditic Orange-Spotted Grouper, Epinephelus coioides. International Journal of Molecular Sciences. 2021;22(22):12607. doi: 10.3390/ijms222212607.

53. Lacerda SMdSN, Costa GMJ, de França LR. Biology and identity of fish spermatogonial stem cell. General and Comparative Endocrinology. 2014;207:56-65. doi: https://doi.org/10.1016/j.ygcen.2014.06.018.

54. Xie X, Nóbrega R, Pšenička M. Spermatogonial Stem Cells in Fish: Characterization, Isolation, Enrichment, and Recent Advances of In Vitro Culture Systems. Biomolecules. 2020;10(4):644. doi: 10.3390/biom10040644.

1358 55. Jin C, Yan K, Wang M, Song W, Wang B, Men Y, et al. Dissecting the dynamic cellular
1359 transcriptional atlas of adult teleost testis development throughout the annual reproductive
1360 cycle. Development. 2024;151(20). doi: 10.1242/dev.202296.
1361 56. Fuess LE, Bolnick DI. Single-Cell RNA Sequencing Reveals Microevolution of the
1362 Stickleback Immune System. Genome Biology and Evolution. 2023;15(4). doi:
1363 10.1093/gbe/evad053.
1364 57. Wolf FA, Angerer P, Theis FJ. SCANPY: large-scale single-cell gene expression data
1365 analysis. Genome Biology. 2018;19(1). doi: 10.1186/s13059-017-1382-0.
1366 58. Hirota T, Blakeley P, Sangrithi MN, Mahadevaiah SK, Encheva V, Snijders AP, et al.
1367 SETDB1 Links the Meiotic DNA Damage Response to Sex Chromosome Silencing in Mice.
1368 Developmental Cell. 2018;47(5):645-59.e6. doi: 10.1016/j.devcel.2018.10.004.
1369 59. Sedelnikova OA, Pilch DR, Redon C, Bonner WM. Histone H2AX in DNA damage and
1370 repair. Cancer Biol Ther. 2003;2(3):233-5. Epub 2003/07/25. doi: 10.4161/cbt.2.3.373. PubMed
1371 PMID: 12878854.
1372 60. Shaw DE, White MA. The evolution of gene regulation on sex chromosomes. Trends in
1373 Genetics. 2022. doi: 10.1016/j.tig.2022.04.004.
1374 61. Beaudry FEG, Barrett SCH, Wright SI. Genomic Loss and Silencing on the Y Chromosomes
1375 of Rumex. Genome Biology and Evolution. 2017;9(12):3345-55. doi: 10.1093/gbe/evx254.
1376 62. Veltsos P, Ridout KE, Toups MA, González-Martínez SC, Muyle A, Emery O, et al. Early
1377 Sex-Chromosome Evolution in the Diploid Dioecious Plant Mercurialis annua. Genetics.
1378 2019;212(3):815-35. doi: 10.1534/genetics.119.302045.
1379 63. Wei KHC, Bachtrog D. Ancestral male recombination in Drosophila albomicans produced
1380 geographically restricted neo-Y chromosome haplotypes varying in age and onset of decay.
1381 PLOS Genetics. 2019;15(11):e1008502. doi: 10.1371/journal.pgen.1008502.
1382 64. Martin H, Carpentier F, Gallina S, Godé C, Schmitt E, Muyle A, et al. Evolution of Young
1383 Sex Chromosomes in Two Dioecious Sister Plant Species with Distinct Sex Determination
1384 Systems. Genome Biology and Evolution. 2019;11(2):350-61. doi: 10.1093/gbe/evz001.
1385 65. Koslowski M, Sahin U, Huber C, Türeci O. The human X chromosome is enriched for
1386 germline genes expressed in premeiotic germ cells of both sexes. Hum Mol Genet.
1387 2006;15(15):2392-9. Epub 2006/07/01. doi: 10.1093/hmg/ddl163. PubMed PMID: 16809397.
1388 66. Shaw DE, Naftaly AS, White MA. Positive Selection Drives cis-regulatory Evolution Across
1389 the Threespine Stickleback Y Chromosome. Molecular Biology and Evolution. 2024;41(2). doi:
1390 10.1093/molbev/msae020.
1391 67. Martínez-Pacheco M, Tenorio M, Almonte L, Fajardo V, Godínez A, Fernández D, et al.
1392 Expression Evolution of Ancestral XY Gametologs across All Major Groups of Placental
1393 Mammals. Genome Biology and Evolution. 2020;12(11):2015-28. doi: 10.1093/gbe/evaa173.
1394 68. Bachtrog D. Y-chromosome evolution: emerging insights into processes of Y-
1395 chromosome degeneration. Nature Reviews Genetics. 2013;14(2):113-24. doi:
1396 10.1038/nrg3366.
1397 69. Cocquet J, Ellis PJI, Mahadevaiah SK, Affara NA, Vaiman D, Burgoyne PS. A Genetic Basis
1398 for a Postmeiotic X Versus Y Chromosome Intragenomic Conflict in the Mouse. PLoS Genetics.
1399 2012;8(9):e1002900. doi: 10.1371/journal.pgen.1002900.

70. Cocquet J, Ellis PJI, Yamauchi Y, Mahadevaiah SK, Affara NA, Ward MA, et al. The Multicopy Gene Sly Represses the Sex Chromosomes in the Male Mouse Germline after Meiosis. PLoS Biology. 2009;7(11):e1000244. doi: 10.1371/journal.pbio.1000244.
71. Bachtrog D, Mahajan S, Bracewell R. Massive gene amplification on a recently formed Drosophila Y chromosome. Nature Ecology & Evolution. 2019;3(11):1587-97. doi: 10.1038/s41559-019-1009-9.
72. Hirano T. At the heart of the chromosome: SMC proteins in action. Nature Reviews Molecular Cell Biology. 2006;7(5):311-22. doi: 10.1038/nrm1909.
73. Moretti C, Vaiman D, Tores F, Cocquet J. Expression and epigenomic landscape of the sex chromosomes in mouse post-meiotic male germ cells. Epigenetics & Chromatin. 2016;9(1). doi: 10.1186/s13072-016-0099-8.
74. Emerson JJ, Kaessmann H, Betrán E, Long M. Extensive Gene Traffic on the Mammalian X Chromosome. Science. 2004;303(5657):537-40. doi: doi:10.1126/science.1090042.
75. Shiao M-S, Khil P, Camerini-Otero RD, Shiroishi T, Moriwaki K, Yu H-T, et al. Origins of New Male Germ-line Functions from X-Derived Autosomal Retrogenes in the Mouse. Molecular Biology and Evolution. 2007;24(10):2242-53. doi: 10.1093/molbev/msm153.
76. Bell MA, Stewart JD, Park PJ. The World's Oldest Fossil Threespine Stickleback Fish. Copeia. 2009;2009(2):256-65. doi: 10.1643/cg-08-059.
77. Ross JA, Urton JR, Boland J, Shapiro MD, Peichel CL. Turnover of Sex Chromosomes in the Stickleback Fishes (Gasterosteidae). PLoS Genetics. 2009;5(2):e1000391. doi: 10.1371/journal.pgen.1000391.
78. Varadharajan S, Rastas P, Löytynoja A, Matschiner M, Calboli FCF, Guo B, et al. A high-quality assembly of the nine-spined stickleback (Pungitius pungitius) genome. Genome Biology and Evolution. 2019. doi: 10.1093/gbe/evz240.
79. Graves JAM. Evolution of vertebrate sex chromosomes and dosage compensation. Nature Reviews Genetics. 2016;17(1):33-46. doi: 10.1038/nrg.2015.2.
80. Mank JE, Ellegren H. All dosage compensation is local: Gene-by-gene regulation of sex-biased expression on the chicken Z chromosome. Heredity. 2009;102(3):312-20. doi: 10.1038/hdy.2008.116.
81. Mullon C, Wright AE, Reuter M, Pomiankowski A, Mank JE. Evolution of dosage compensation under sexual selection differs between X and Z chromosomes. Nature Communications. 2015;6(1):7720. doi: 10.1038/ncomms8720.
82. Wei KHC, Chatla K, Bachtrog D. Single-cell RNA-seq of Drosophila miranda testis reveals the evolution and trajectory of germline sex chromosome regulation. PLOS Biology. 2024;22(4):e3002605. doi: 10.1371/journal.pbio.3002605.
83. Witt E, Shao Z, Hu C, Krause HM, Zhao L. Single-cell RNA-sequencing reveals pre-meiotic X-chromosome dosage compensation in Drosophila testis. PLOS Genetics. 2021;17(8):e1009728. doi: 10.1371/journal.pgen.1009728.
84. Mrnjavac A, Khudiakova KA, Barton NH, Vicoso B. Slower-X: reduced efficiency of selection in the early stages of X chromosome evolution. Evolution Letters. 2023;7(1):4-12. doi: 10.1093/evlett/qrac004.
85. Nath S, Shaw DE, White MA. Improved contiguity of the threespine stickleback genome using long-read sequencing. G3 Genes|Genomes|Genetics. 2021;11(2). doi: 10.1093/g3journal/jkab007.

1444 86. Wang D, Rastas P, Yi X, Löytynoja A, Kivikoski M, Feng X, et al. Improved assembly of the
1445 Pungitius pungitius reference genome. G3 Genes|Genomes|Genetics. 2024;14(8). doi:
1446 10.1093/g3journal/jkae126.
1447 87. Good JM, Nachman MW. Rates of protein evolution are positively correlated with
1448 developmental timing of expression during mouse spermatogenesis. Mol Biol Evol.
1449 2005;22(4):1044-52. Epub 2005/01/14. doi: 10.1093/molbev/msi087. PubMed PMID:
1450 15647515.
1451 88. Kopania EEK, Larson EL, Callahan C, Keeble S, Good JM. Molecular Evolution across
1452 Mouse Spermatogenesis. Molecular Biology and Evolution. 2022;39(2). doi:
1453 10.1093/molbev/msac023.
1454 89. Larson EL, Vanderpool D, Keeble S, Zhou M, Sarver BA, Smith AD, et al. Contrasting
1455 Levels of Molecular Evolution on the Mouse X Chromosome. Genetics. 2016;203(4):1841-57.
1456 Epub 2016/06/19. doi: 10.1534/genetics.116.186825. PubMed PMID: 27317678; PubMed
1457 Central PMCID: PMCPMC4981281.
1458 90. Lifschytz E, Lindsley DL. The role of X-chromosome inactivation during spermatogenesis.
1459 Proceedings of the National Academy of Sciences. 1972;69(1):182-6.
1460 91. McKee BD, Handel MA. Sex chromosomes, recombination, and chromatin conformation.
1461 Chromosoma. 1993;102(2):71-80. doi: 10.1007/BF00356023.
1462 92. Solari AJ. Equalization of Z and W axes in chicken and quail oocytes. Cytogenet Cell
1463 Genet. 1992;59(1):52-6. Epub 1992/01/01. doi: 10.1159/000133199. PubMed PMID: 1733674.
1464 93. Meiklejohn CD, Tao Y. Genetic conflict and sex chromosome evolution. Trends in
1465 Ecology & Evolution. 2010;25(4):215-23. doi: 10.1016/j.tree.2009.10.005.
1466 94. Wu C-I, Yujun Xu E. Sexual antagonism and X inactivation – the SAXI hypothesis. Trends
1467 in Genetics. 2003;19(5):243-7. doi: 10.1016/s0168-9525(03)00058-1.
1468 95. Good JM. The Conflict within and the Escalating War between the Sex Chromosomes.
1469 PLoS Genetics. 2012;8(9):e1002955. doi: 10.1371/journal.pgen.1002955.
1470 96. Casey AE, Daish TJ, Barbero JL, Grützner F. Differential cohesin loading marks paired and
1471 unpaired regions of platypus sex chromosomes at prophase I. Scientific Reports.
1472 2017;7(1):4217. doi: 10.1038/s41598-017-04560-5.
1473 97. Schoenmakers S, Wassenaar E, Hoogerbrugge JW, Laven JSE, Grootegoed JA, Baarends
1474 WM. Female Meiotic Sex Chromosome Inactivation in Chicken. PLoS Genetics.
1475 2009;5(5):e1000466. doi: 10.1371/journal.pgen.1000466.
1476 98. Namekawa SH, Lee JT. XY and ZW: is meiotic sex chromosome inactivation the rule in
1477 evolution? PLoS Genet. 2009;5(5):e1000493. Epub 2009/05/23. doi:
1478 10.1371/journal.pgen.1000493. PubMed PMID: 19461890; PubMed Central PMCID:
1479 PMCPMC2679206.
1480 99. Vibranovski MD, Lopes HF, Karr TL, Long M. Stage-Specific Expression Profiling of
1481 Drosophila Spermatogenesis Suggests that Meiotic Sex Chromosome Inactivation Drives
1482 Genomic Relocation of Testis-Expressed Genes. PLoS Genetics. 2009;5(11):e1000731. doi:
1483 10.1371/journal.pgen.1000731.
1484 100. Mahadevaraju S, Fear JM, Akeju M, Galletta BJ, Pinheiro MMLS, Avelino CC, et al.
1485 Dynamic sex chromosome expression in Drosophila male germ cells. Nature Communications.
1486 2021;12(1). doi: 10.1038/s41467-021-20897-y.

101. Vibranovski MD. Meiotic sex chromosome inactivation in Drosophila. J Genomics. 2014;2:104-17. Epub 2014/07/25. doi: 10.7150/jgen.8178. PubMed PMID: 25057326; PubMed Central PMCID: PMCPMC4105432.
102. Viera A, Parra MT, Arévalo S, García De La Vega C, Santos JL, Page J. X Chromosome Inactivation during Grasshopper Spermatogenesis. Genes. 2021;12(12):1844. doi: 10.3390/genes12121844.
103. Page N, Taxiarchi C, Tonge D, Kuburic J, Chesters E, Kriezis A, et al. Single-cell profiling of Anopheles gambiae spermatogenesis defines the onset of meiotic silencing and premeiotic overexpression of the X chromosome. Communications Biology. 2023;6(1):850. doi: 10.1038/s42003-023-05224-z.
104. Taxiarchi C, Kranjc N, Kriezis A, Kyrou K, Bernardini F, Russell S, et al. High-resolution transcriptional profiling of Anopheles gambiae spermatogenesis reveals mechanisms of sex chromosome regulation. Scientific Reports. 2019;9(1). doi: 10.1038/s41598-019-51181-1.
105. Lisachov A, Dedukh D, Simanovsky S, Panthum T, Singchat W, Srikulnath K. Spaghetti Connections: Synaptonemal Complexes as a Tool to Explore Chromosome Structure, Evolution, and Meiotic Behavior in Fish. Cytogenet Genome Res. 2024;164(1):1-15. Epub 2024/03/08. doi: 10.1159/000538238. PubMed PMID: 38452741.
106. Nanda I, Schories S, Simeonov I, Adolfi MC, Du K, Steinlein C, et al. Evolution of the Degenerated Y-Chromosome of the Swamp Guppy, Micropoecilia picta. Cells. 2022;11(7). Epub 2022/04/13. doi: 10.3390/cells11071118. PubMed PMID: 35406682; PubMed Central PMCID: PMCPMC8997885.
107. Bachtrog D. The Y Chromosome as a Battleground for Intragenomic Conflict. Trends Genet. 2020;36(7):510-22. Epub 2020/05/26. doi: 10.1016/j.tig.2020.04.008. PubMed PMID: 32448494; PubMed Central PMCID: PMCPMC8329999.
108. Mank JE, Hosken DJ, Wedell N. Conflict on the sex chromosomes: cause, effect, and complexity. Cold Spring Harb Perspect Biol. 2014;6(12):a017715. Epub 2014/10/05. doi: 10.1101/cshperspect.a017715. PubMed PMID: 25280765; PubMed Central PMCID: PMCPMC4292157.
109. Chang C-H, Gregory LE, Gordon KE, Meiklejohn CD, Larracuente AM. Unique structure and positive selection promote the rapid divergence of Drosophila Y chromosomes. eLife. 2022;11. doi: 10.7554/elife.75795.
110. Lin Y, Darolti I, Furman BLS, Almeida P, Sandkam BA, Breden F, et al. Gene duplication to the Y chromosome in Trinidadian Guppies. Molecular Ecology. 2022;31(6):1853-63. doi: 10.1111/mec.16355.
111. Moretti C, Blanco M, Ialy-Radio C, Serrentino ME, Gobé C, Friedman R, et al. Battle of the Sex Chromosomes: Competition between X and Y Chromosome-Encoded Proteins for Partner Interaction and Chromatin Occupancy Drives Multicopy Gene Expression and Evolution in Muroid Rodents. Mol Biol Evol. 2020;37(12):3453-68. Epub 2020/07/14. doi: 10.1093/molbev/msaa175. PubMed PMID: 32658962; PubMed Central PMCID: PMCPMC7743899.
112. Mueller JL, Skaletsky H, Brown LG, Zaghlul S, Rock S, Graves T, et al. Independent specialization of the human and mouse X chromosomes for the male germ line. Nature Genetics. 2013;45(9):1083-7. doi: 10.1038/ng.2705.

113. Liu J, Shikano T, Leinonen T, Cano JM, Li M-H, Merilä J. Identification of Major and Minor QTL for Ecologically Important Morphological Traits in Three-Spined Sticklebacks (Gasterosteus aculeatus). G3 Genes|Genomes|Genetics. 2014;4(4):595-604. doi: 10.1534/g3.114.010389.
114. Rollins JL, Chiang P, Waite JN, Von Hippel FA, Bell MA. Jacks and jills: Alternative life-history phenotypes and skewed sex ratio in anadromous threespine stickleback (Gasterosteus aculeatus). Evolutionary Ecology Research. 2017;18(4):363-82.
115. Chang C-H, Mejia Natividad I, Malik HS. Expansion and loss of sperm nuclear basic protein genes in Drosophila correspond with genetic conflicts between sex chromosomes. eLife. 2023;12:e85249. doi: 10.7554/eLife.85249.
116. Larracuente AM, Presgraves DC. The SelfishSegregation DistorterGene Complex ofDrosophila melanogaster. Genetics. 2012;192(1):33-53. doi: 10.1534/genetics.112.141390.
117. Ellis PJI, Bacon J, Affara NA. Association of Sly with sex-linked gene amplification during mouse evolution: a side effect of genomic conflict in spermatids? Human Molecular Genetics. 2011;20(15):3010-21. doi: 10.1093/hmg/ddr204.
118. Olds-Clarke P. Models for male infertility: the t haplotypes. Rev Reprod. 1997;2(3):157-64. Epub 1998/01/01. doi: 10.1530/ror.0.0020157. PubMed PMID: 9414479.
119. Phadnis N, Orr HA. A Single Gene Causes Both Male Sterility and Segregation Distortion in Drosophila Hybrids. Science. 2009;323(5912):376-9. doi: 10.1126/science.1163934.
120. Fitzpatrick JL. Sperm competition and fertilization mode in fishes. Philosophical Transactions of the Royal Society B: Biological Sciences. 2020;375(1813):20200074. doi: 10.1098/rstb.2020.0074.
121. Verspoor RL, Price TAR, Wedell N. Selfish genetic elements and male fertility. Philos Trans R Soc Lond B Biol Sci. 2020;375(1813):20200067. Epub 2020/10/20. doi: 10.1098/rstb.2020.0067. PubMed PMID: 33070738; PubMed Central PMCID: PMCPMC7661447.
122. Van den Assem J. Territory in the three-spined stickleback Gasterosteus aculeatus L.: an experimental study in intra-specific competition: Brill Archive; 1967.
123. Largiadèr CR, Fries V, Bakker TCM. Genetic analysis of sneaking and egg-thievery in a natural population of the three-spined stickleback (Gasterosteus aculeatus L.). Heredity. 2001;86(4):459-68. doi: 10.1046/j.1365-2540.2001.00850.x.
124. Hao Y, Hao S, Andersen-Nissen E, Mauck WM, Zheng S, Butler A, et al. Integrated analysis of multimodal single-cell data. Cell. 2021;184(13):3573-87.e29. doi: 10.1016/j.cell.2021.04.048.
125. Sokołowska E, Kulczykowska E. Annual reproductive cycle in two free living populations of three-spined stickleback (Gasterosteus aculeatus L.): Patterns of ovarian and testicular development. Oceanologia. 2006;48.
126. Borg B. Effects of methyltestosterone on spermatogenesis and secondary sexual characters in the three-spined stickleback (Gasterosteus aculeatus L.). General and Comparative Endocrinology. 1981;44(2):177-80. doi: 10.1016/0016-6480(81)90245-8.
127. Dapper AL, Payseur BA. Molecular evolution of the meiotic recombination pathway in mammals. Evolution. 2019;73(12):2368-89. doi: 10.1111/evo.13850.
128. Anders S, Pyl PT, Huber W. HTSeq--a Python framework to work with high-throughput sequencing data. Bioinformatics. 2015;31(2):166-9. doi: 10.1093/bioinformatics/btu638.

1573 129. Cunningham F, Allen JE, Allen J, Alvarez-Jarreta J, Amode M R, Armean Irina M, et al.
1574 Ensembl 2022. Nucleic Acids Research. 2021;50(D1):D988-D95. doi: 10.1093/nar/gkab1049.
1575 130. Slater GSC, Birney E. Automated generation of heuristics for biological sequence
1576 comparison. BMC Bioinformatics. 2005;6(1):31. doi: 10.1186/1471-2105-6-31.
1577 131. Yang Z. PAML 4: Phylogenetic Analysis by Maximum Likelihood. Molecular Biology and
1578 Evolution. 2007;24(8):1586-91. doi: 10.1093/molbev/msm088.
1579 132. Blokhina YP, Nguyen AD, Draper BW, Burgess SM. The telomere bouquet is a hub where
1580 meiotic double-strand breaks, synapsis, and stable homolog juxtaposition are coordinated in
1581 the zebrafish, Danio rerio. PLoS Genet. 2019;15(1):e1007730. Epub 2019/01/18. doi:
1582 10.1371/journal.pgen.1007730. PubMed PMID: 30653507; PubMed Central PMCID:
1583 PMCPMC6336226.
1584

1585

1586 **Supplemental Figure 1. Gene counts per samples.**

1587 Number of transcripts detected for each gene was totaled for each cell barcode within each of the
1588 three single cell RNA sequencing experiments. A similar distribution of detected genes were
1589 identified in each of three experiments.

1590
1591
1592

1593 **Supplemental Figure 2. Clusters split by sequencing replicate.** Cell barcodes from all three
1594 sequencing runs were merged, and UMAP is depicted for all merged cells (top), and for each
1595 replicate separately (bottom). Proportion of each cell type within each sample was dependent on
1596 the onset of synchronous spermatogenesis in each individual. Only cell clusters identified in two
1597 of three replicates were used for downstream analysis.

1598
1599

1600 **Supplemental Figure 3. Cluster wide expression correlation across all samples.** Normalized
1601 gene expression of the top 500 expressed genes in each cluster was averaged and compared for

1602 each cluster and sample. Hierarchical clustering reveals that most clusters cluster by cell types

1603 across replicates rather than by sample.

1604
1605
1606
1607
1608

1609 **Supplemental Figure 4. Marker genes for all clusters.** Differentially expressed genes in each

1610 cell cluster correspond with diverse testis cell types. Heatmap was generated for the top 250

1611 variable expressed genes across all clusters. Represented marker genes for each cluster are listed

1612 in boxes. Clusters were assigned to five major cell groups for downstream analysis.based on

1613 similar expression and biological functions . Bottom: Cluster dotplots for representative marker

1614 genes. Marker genes were identified based on having significantly different expression ($P < 0.01$,

1615 Mann-Whitney U test), and had a confirmed function in the cell type in other species.

1616

1617

1618 **Supplemental Figure 5. Correlation of cluster expression profiles across replicates**

1619 Gene expression for all expressed genes identified in clusters were highly correlated ($R > 0.69$)

1620 across samples. Testis 2 and 3 showed stronger correlations across cell types compared to s,

1621 likely due to a similar developmental staging at the time of testis dissociation. Spearman rank

1622 correlation is reported above each graph. Cell types are noted as Pre (pre-meiotic), M (meiotic),

1623 Pst (post-meiotic), and Som (somatic).

1624

1625

1626 **Supplemental Figure 6. X:AA expression across all clusters and samples**

1627 No evidence for MSCI across all three samples when examining all identified clusters. X gene
1628 expression was normalized by autosomal gene expression for each cluster across all three
1629 samples. Letters denote statistical significance based on a Kruskal Wallis test and Dunn's test.
1630 Dotted line represents median X:A expression level across main cell groups in Figure 2.
1631
1632
1633
1634 **Supplemental Figure 7. Broadly expressed genes are maintained across all stages of**
1635 **spermatogenesis.** Bulk RNA-seq data from three tissues brain, liver, and testis were compared
1636 to identify genes that were expressed testis specifically. When we filtered out 20 testis specific
1637 X-linked genes, we still identify similar expression across all stages of spermatogenesis $P > 0.05$
1638 for all comparisons, Kruskal-Wallis and Dunn's test.
1639
1640
1641
1642
1643 **Supplemental Figure 8. Lack of MSCI is robust across distinct cell clustering algorithms**
1644 **and software.** Top: Normalized X expression was compared between two distinct clustering
1645 algorithms in Seurat. X expression was similar across major cell groups for both algorithms ($P =$
1646 0.441, Kruskal Wallis test. Bottom: Cell clustering was reanalyzed with a separate software
1647 package (scanpy) and re-annotated using cell markers. Scanpy clustering was performed using
1648 all three samples. Normalized X expression is similar across all stages of spermatogenesis. Only
1649 two somatic clusters had variable expression ($P < 0.05$, Kruskal wallis and Dunn's test).

1650

1651

1652 **Supplemental Figure 9. Enrichment of X- and Y- mono-allelic expressed genes across**

1653 **stages of spermatogenesis.** Gametolog specific expression was identified for the 4 main cell

1654 types of spermatogenesis by aggregated counts from all clusters. Genes with transcripts aligned

1655 to only one sex chromosome per cluster were identified. Mono-allelic expression was confirmed

1656 using bulk RNA-seq from three replicates of meiotically active testis. Enrichment of mono-

1657 allelic expression across cell stages was calculated using a hypergeometirc test comparing the

1658 number of mono-allelic expressed genes observed to expected based on the number of genes

1659 expressed in that cell type. X- only expression was overenriched in pre-meiotic cells ($P < 0.01$).

1660 Y-only expression was over-enriched in pre-meiotic and post-meiotic cell types ($P < 0.01$), and

1661 under-enriched in meiotic cell types ($P < 0.01$).

1662

1663 **Supplemental Figure 10.** d_N/d_S **across all induced genes in major cell groups of**

1664 **spermatogenesis.** d_N/d_S was calculated between ninespine and threespine stickleback for genes

1665 on autosomes, X hemizygous genes, X and Y gametologs, and Y homozygous genes. scRNA-seq

1666 was used to identify genes that were induced in four major cell groups. Letters denote statistical

1667 comparisons across all remaining stages and categories based on Kruskal Wallis and Dunn's

1668 test. Autosomes have the highest count with 2,262 genes followed by X hemizygous genes with

1669 50 genes, X gametologs with 31 genes, Y gametologs with 31 genes, and Y hemizygous genes

1670 with just 4 genes.

1671

1672 **Supplemental Figure 11.** d_N/d_S **between threespine and ninespine stickleback for all**
1673 **chromosomes.** Both X gametologs and Chr 12 (Ninespine sex chromosomes) have lower dN/dS
1674 than median autosomal ($P < 0.01$, Kruskal Wallis and Dunn's test). All other comparisons are
1675 not statistically different ($P > 0.05$ for all pairwise comparisons).
1676
1677
1678 **Supplemental Figure 12. Similar signatures of selection across spermatogenesis.** d_N/d_S was
1679 calculated between ninespine and threespine stickleback for genes on autosomes, X hemizygous
1680 genes, X and Y gametologs, and Y homozygous genes. scRNA-seq was used to identify 2378
1681 genes that were induced in four major cell groups. There were no significant differences between
1682 stages for each chromosome group ($P = 0.501$ Kruskal Wallis and Dunn's test). The dataset
1683 includes genes that were induced and had an alignment between threespine and ninespine
1684 stickleback cross four developmental stages for each chromosome category. Autosomes have the
1685 largest sample sizes, with 414, 465, 340, and 1,043 genes across the four stages, respectively. X
1686 gametologs include 16, 3, 5, and 7 genes; X-only genes have 24, 9, 9, and 8 genes; Y gametologs
1687 consist of 16, 3, 5, and 7 genes; and Y-only genes are the smallest group, with just 2 genes in
1688 each of the last two stages.
1689
1690 **Supplemental Figure 13. Identification of significant principal components for scRNA-seq**
1691 Elbow plots and jackstraw simulations were generated to assess the number of significant
1692 principle components for each sequencing experiment.
1693
1694
1695
1696 **Supplemental Figure 14. Number of reads per cell type.**

1697 Number of RNA molecules identified per cell within each cell cluster were counted using Seurat.
1698

1699

1700 **Supplemental File 1. List of all differentially expressed genes identified for each cell type.**

1701 **Supplemental File 2. List of all annotated Y genes and coordinates.**

1702

1703

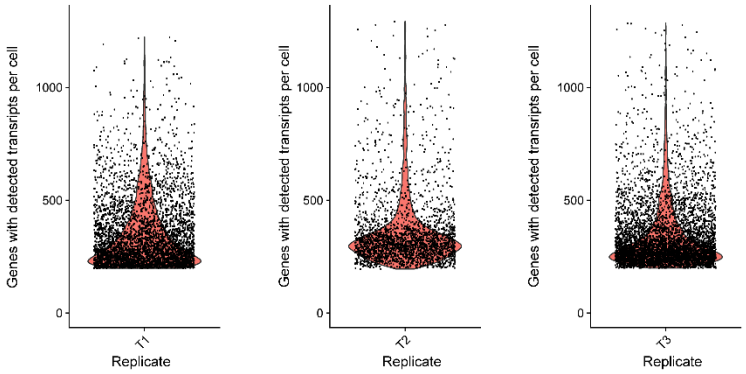

1704

1705 **Supplemental Figure 1. Gene counts per samples.**

1706 Number of transcripts detected for each gene was totaled for each cell barcode within each of the
1707 three single cell RNA sequencing experiments. A similar distribution of detected genes were
1708 identified in each of three experiments.
1709

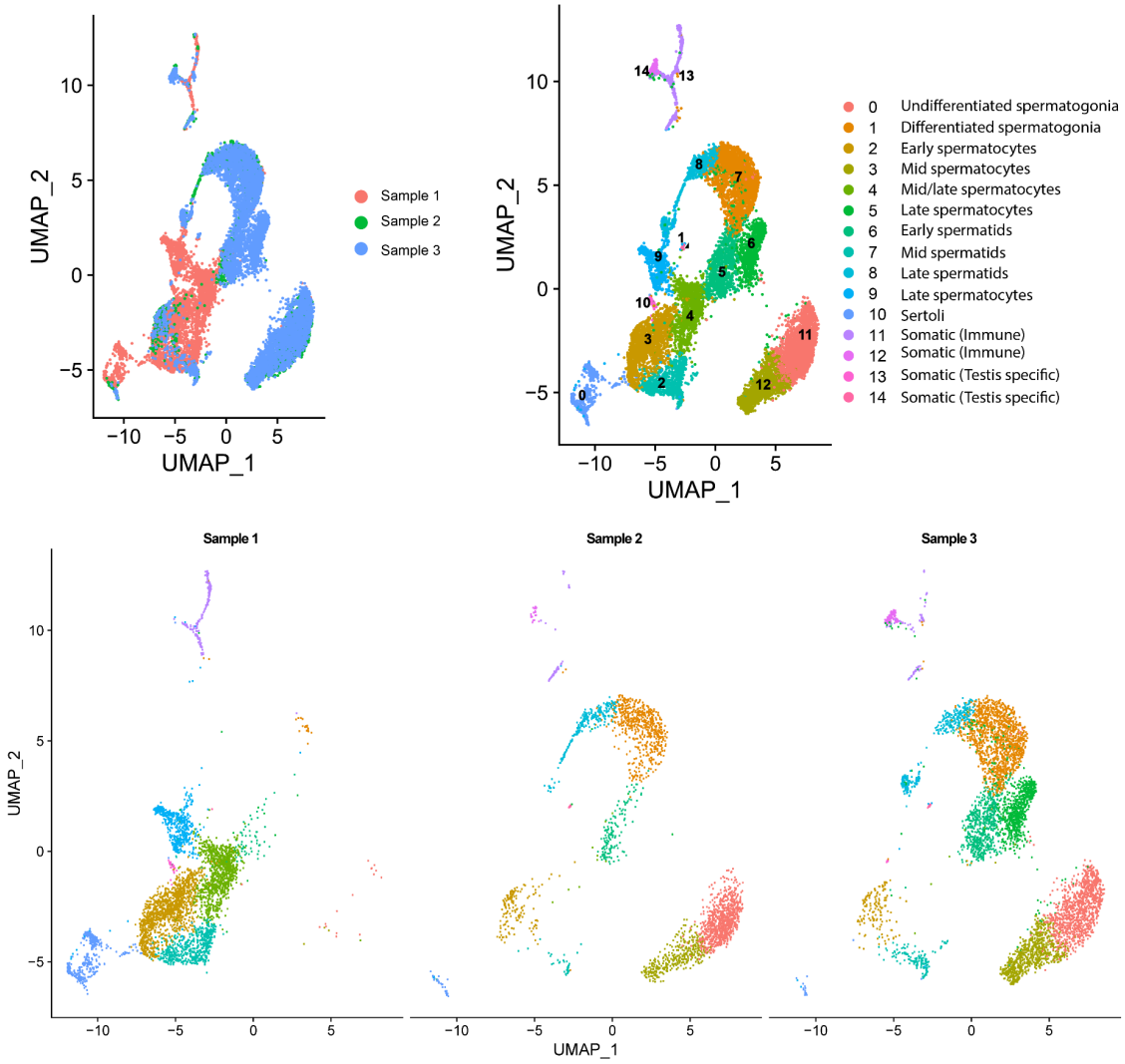

Supplemental Figure 2. Clusters split by sequencing replicate. Cell barcodes from all three sequencing runs were merged, and UMAP is depicted for all merged cells (top), and for each replicate separately (bottom). Proportion of each cell type within each sample was dependent on the onset of synchronous spermatogenesis in each individual. Only cell clusters identified in two of three replicates were used for downstream analysis.

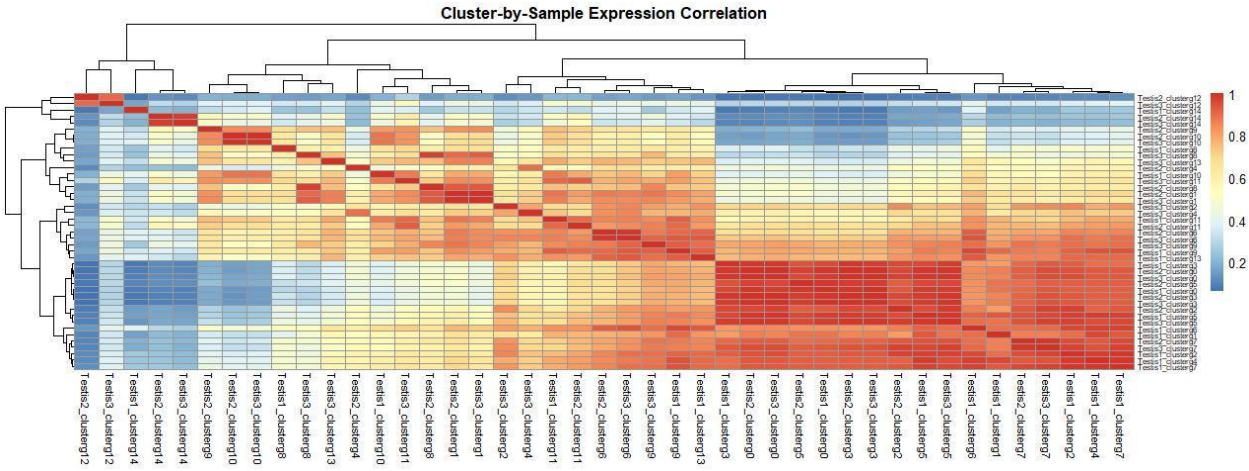

Supplemental Figure 3. Cluster wide expression correlation across all samples. Normalized gene expression of the top 500 expressed genes in each cluster was averaged and compared for each cluster and sample. Hierarchical clustering reveals that most clusters cluster by cell types across replicates rather than by sample.

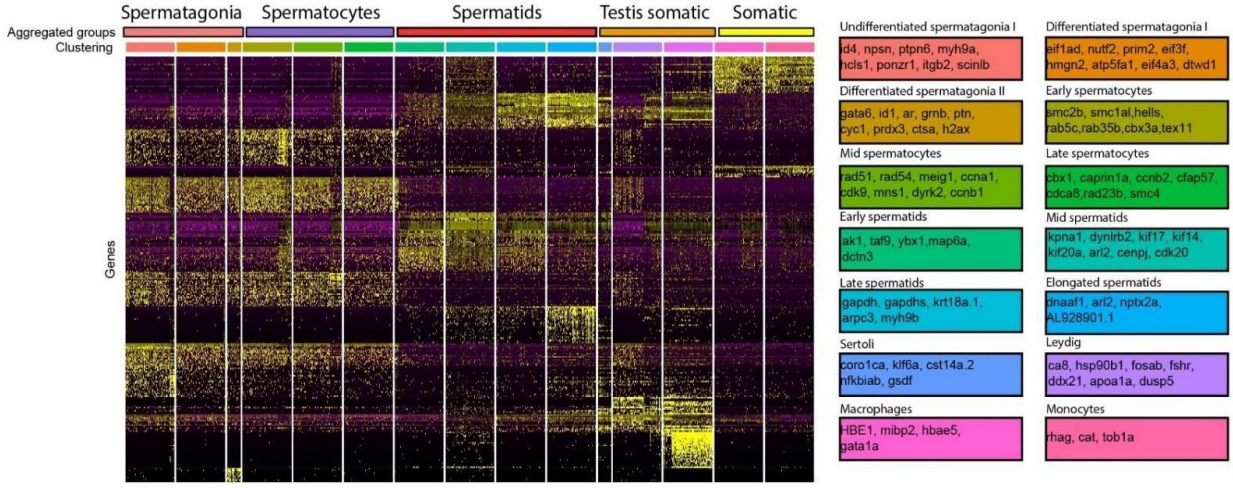

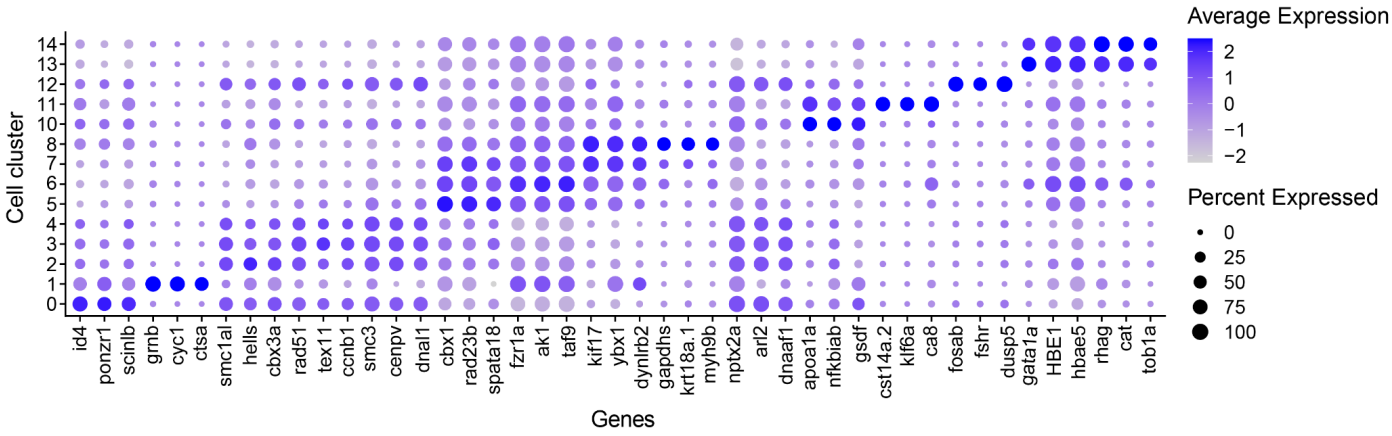

Supplemental Figure 4. Marker genes for all clusters. Differentially expressed genes in each cell cluster correspond with diverse testis cell types. Heatmap was generated for the top 250 variable expressed genes across all clusters. Represented marker genes for each cluster are listed in boxes. Clusters were assigned to five major cell groups for downstream analysis.based on similar expression and biological functions . Bottom: Cluster dotplots for representative marker genes. Marker genes were identified based on having significantly different expression ($P < 0.01$, Mann-Whitney U test), and had a confirmed function in the cell type in other species.

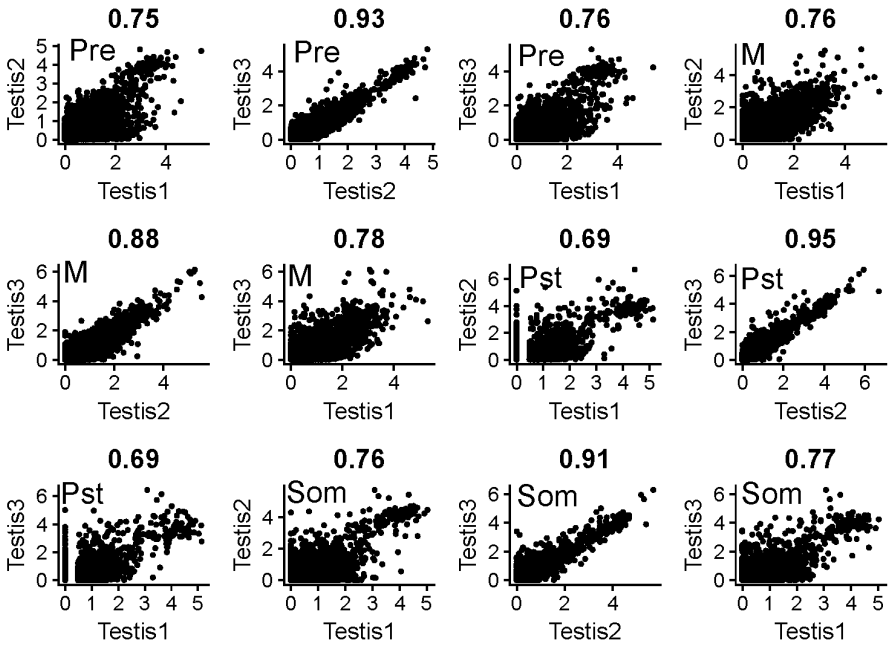

Supplemental Figure 5. Correlation of cluster expression profiles across replicates

Gene expression for all expressed genes identified in clusters were highly correlated (R > 0.69) across samples. Testis 2 and 3 showed stronger correlations across cell types compared to s, likely due to a similar developmental staging at the time of testis dissociation. Spearman rank correlation is reported above each graph. Cell types are noted as Pre (pre-meiotic), M (meiotic), Pst (post-meiotic), and Som (somatic).

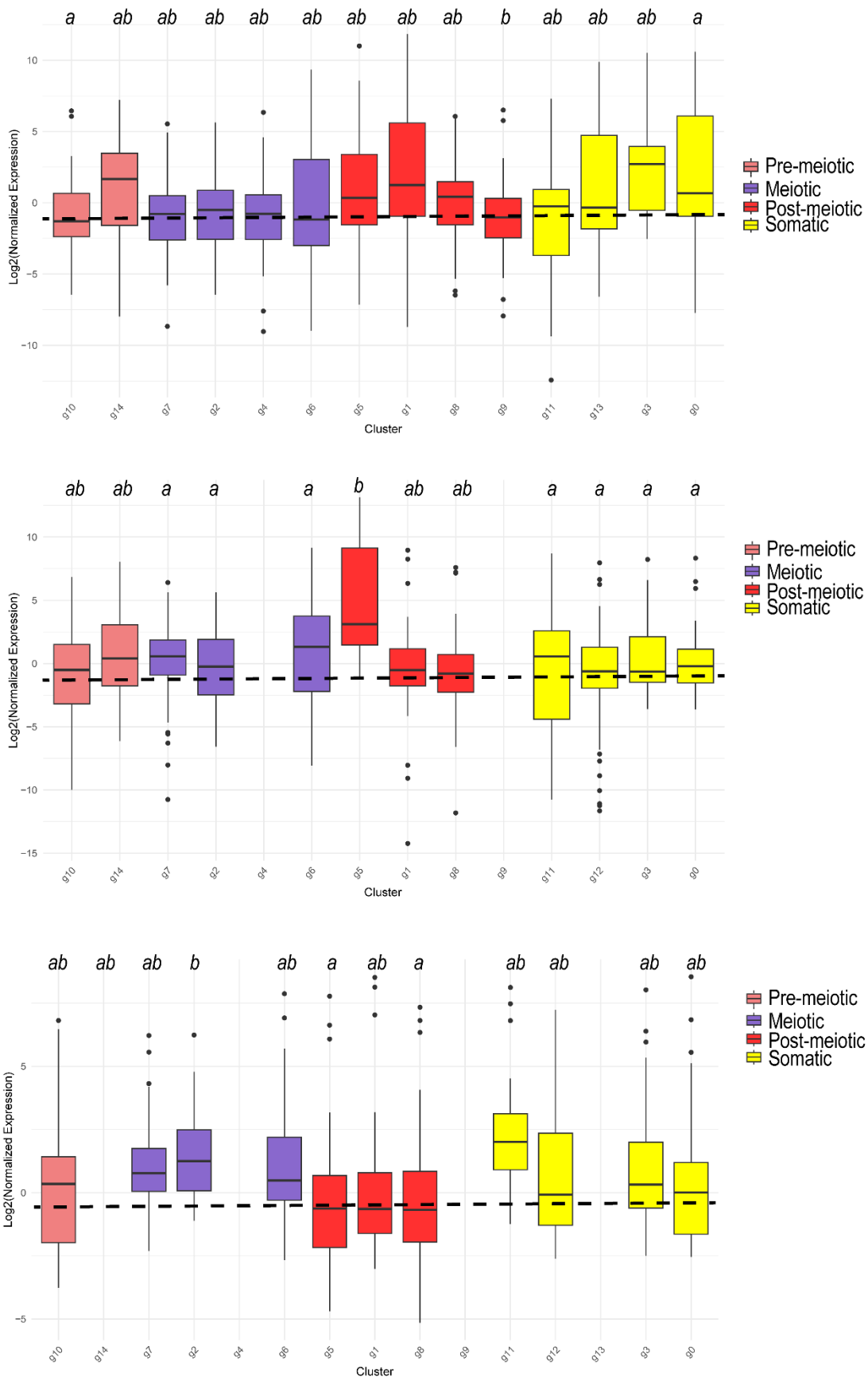
a ab ab ab ab ab ab ab ab b ab ab ab a
Log2(Normalized Expression)
10
5
0
−5
−10
g10 g14 g7 g2 g4 g6 g5 g1 g8 g9 g11 g13 g3 g0
Cluster
Pre-meiotic
Meiotic
Post-meiotic
Somatic
ab ab a a a b ab ab a a a a
Log2(Normalized Expression)
10
5
0
−5
−10
−15
g10 g14 g7 g2 g4 g6 g5 g1 g8 g9 g11 g12 g3 g0
Cluster
Pre-meiotic
Meiotic
Post-meiotic
Somatic
ab ab ab b ab a ab a ab ab ab ab
Log2(Normalized Expression)
5
0
−5
g10 g14 g7 g2 g4 g6 g5 g1 g8 g9 g11 g12 g13 g3 g0
Cluster
Pre-meiotic
Meiotic
Post-meiotic
Somatic

1755

1756 **Supplemental Figure 6. X:AA expression across all clusters and samples**

1757 No evidence for MSCI across all three samples when examining all identified clusters. X gene
1758 expression was normalized by autosomal gene expression for each cluster across all three
1759 samples. Letters denote statistical significance based on a Kruskal Wallis test and Dunn's test.
1760 Dotted line represents median X:A expression level across main cell groups in Figure 2.

1761

1762

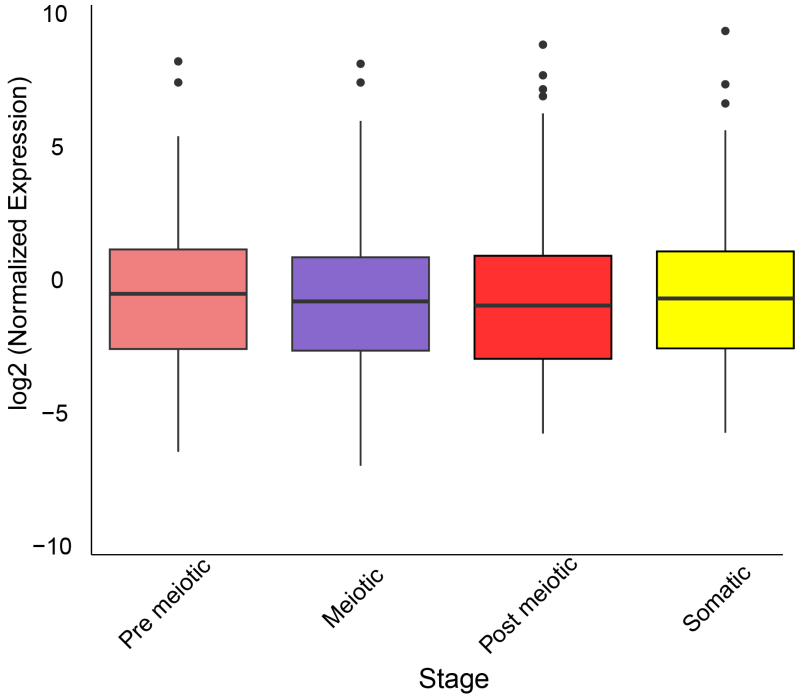

1763

1764 **Supplemental Figure 7. Broadly expressed genes are maintained across all stages of**
1765 **spermatogenesis.** Bulk RNA-seq data from three tissues brain, liver, and testis were compared
1766 to identify genes that were expressed testis specifically. When we filtered out 20 testis specific
1767 X-linked genes, we still identify similar expression across all stages of spermatogenesis $P > 0.05$
1768 for all comparisons, Kruskal-Wallis and Dunn's test.

1769

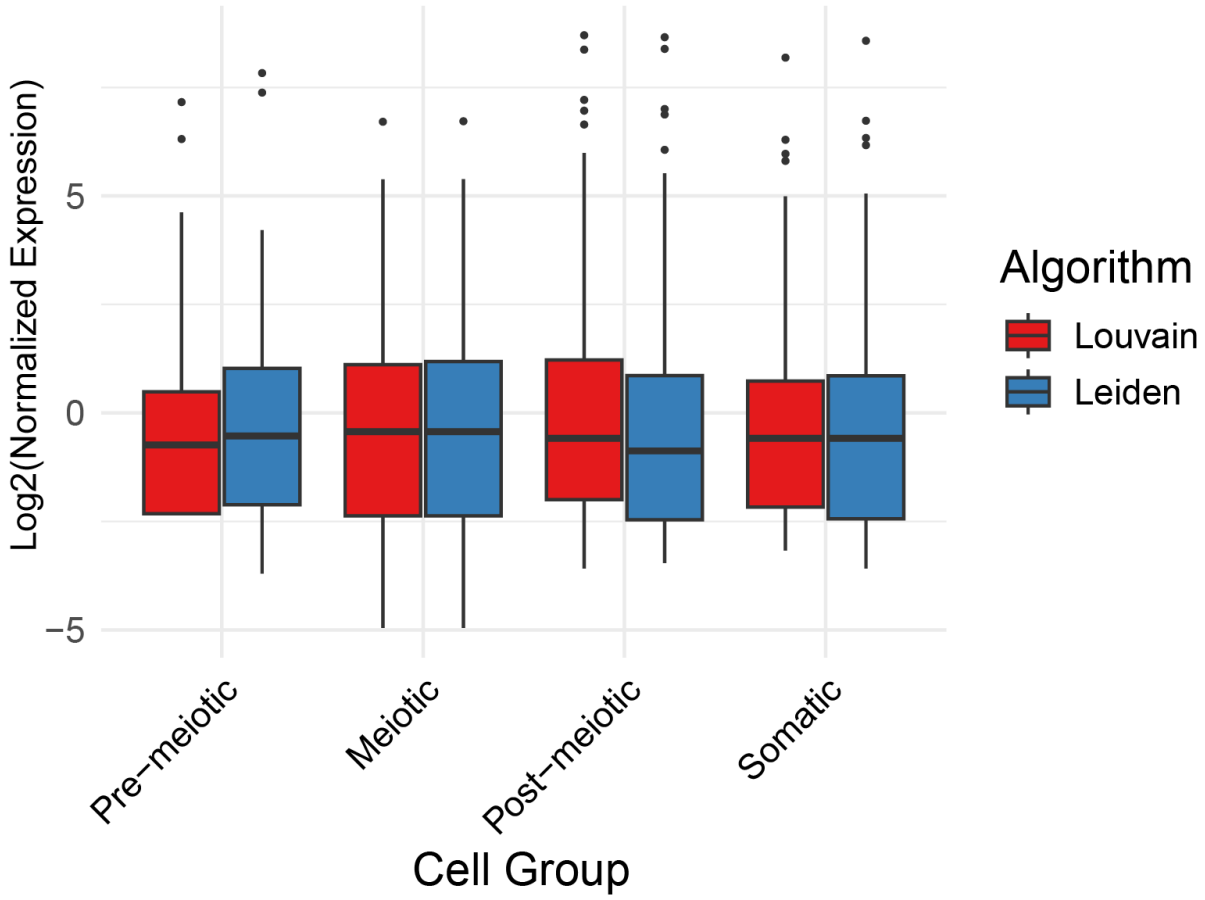

1770

1771

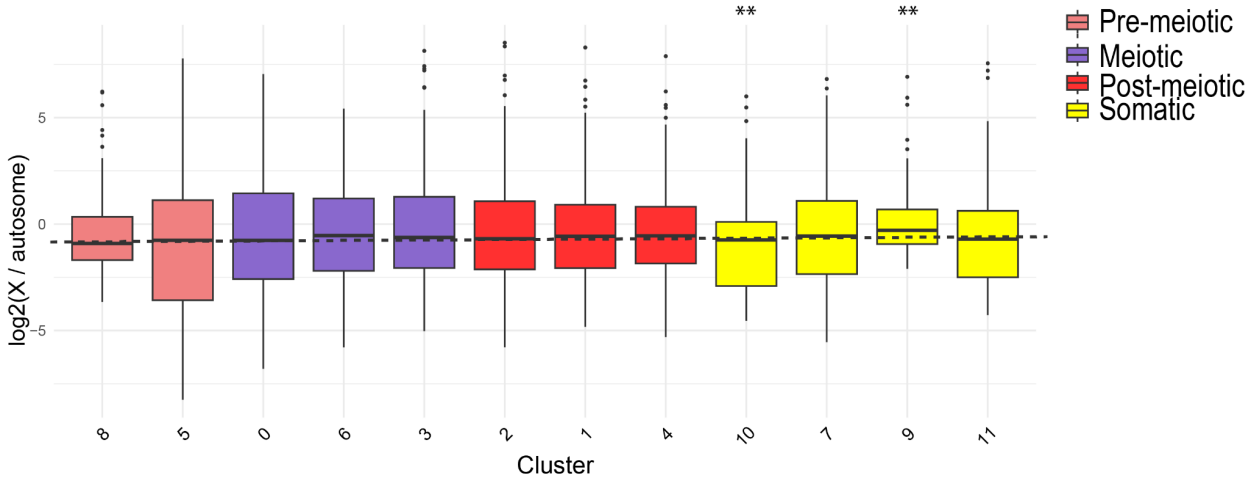

1772

1773 **Supplemental Figure 8. Lack of MSCI is robust across distinct cell clustering algorithms**
1774 **and software.** Top: Normalized X expression was compared between two distinct clustering
1775 algorithms in Seurat. X expression was similar across major cell groups for both algorithms (P =
1776 0.441, Kruskal Wallis test. Bottom: Cell clustering was reanalyzed with a separate software
1777 package (scanpy) and re-annotated using cell markers. Scanpy clustering was performed using
1778 all three samples. Normalized X expression is similar across all stages of spermatogenesis. Only
1779 two somatic clusters had variable expression (P < 0.05, Kruskal wallis and Dunn's test).
1780
1781
1782

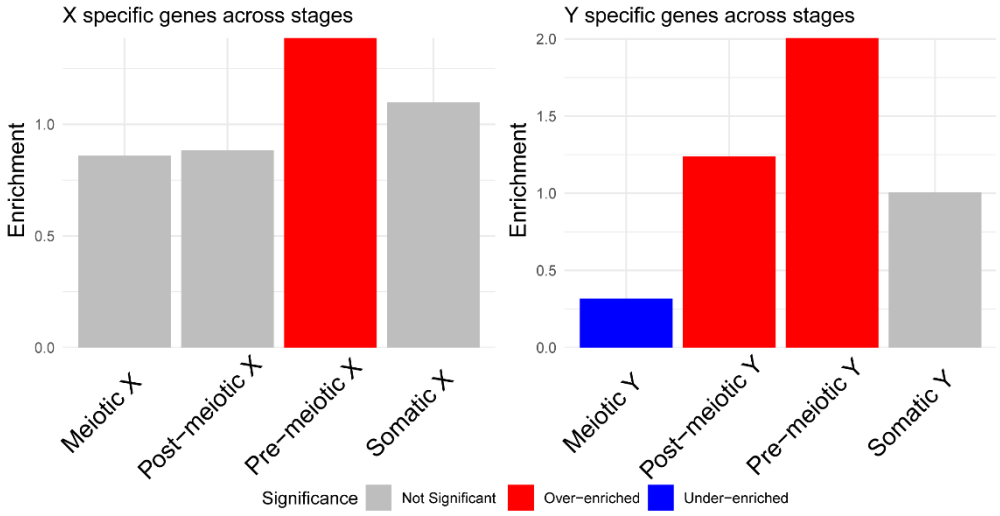

1783
1784 **Supplemental Figure 9. Enrichment of X- and Y- mono-allelic expressed genes across**
1785 **stages of spermatogenesis.** Gametolog specific expression was identified for the 4 main cell
1786 types of spermatogenesis by aggregated counts from all clusters. Genes with transcripts aligned
1787 to only one sex chromosome per cluster were identified. Mono-allelic expression was confirmed
1788 using bulk RNA-seq from three replicates of meiotically active testis. Enrichment of mono-
1789 allelic expression across cell stages was calculated using a hypergeometirc test comparing the

1790 number of mono-allelic expressed genes observed to expected based on the number of genes

1791 expressed in that cell type. X- only expression was overenriched in pre-meiotic cells ($P < 0.01$).

1792 Y-only expression was over-enriched in pre-meiotic and post-meiotic cell types ($P < 0.01$), and

1793 under-enriched in meiotic cell types ($P < 0.01$).

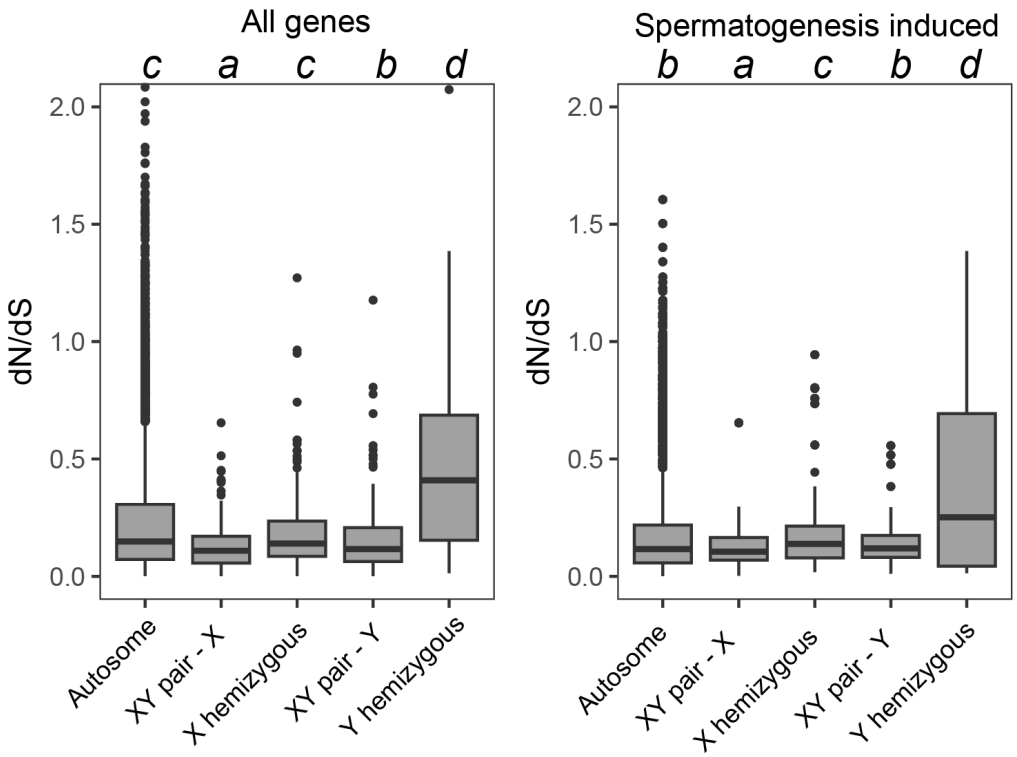

1794

1795 **Supplemental Figure 10.** d_N/d_S **across all induced genes in major cell groups of**

1796 **spermatogenesis.** d_N/d_S was calculated between ninespine and threespine stickleback for genes

1797 on autosomes, X hemizygous genes, X and Y gametologs, and Y homozygous genes. scRNA-seq

1798 was used to identify genes that were induced in four major cell groups. Letters denote statistical

1799 comparisons across all remaining stages and categories based on Kruskal Wallis and Dunn's

1800 test. Autosomes have the highest count with 2,262 genes followed by X hemizygous genes with

1801 50 genes, X gametologs with 31 genes, Y gametologs with 31 genes, and Y hemizygous genes

1802 with just 4 genes.

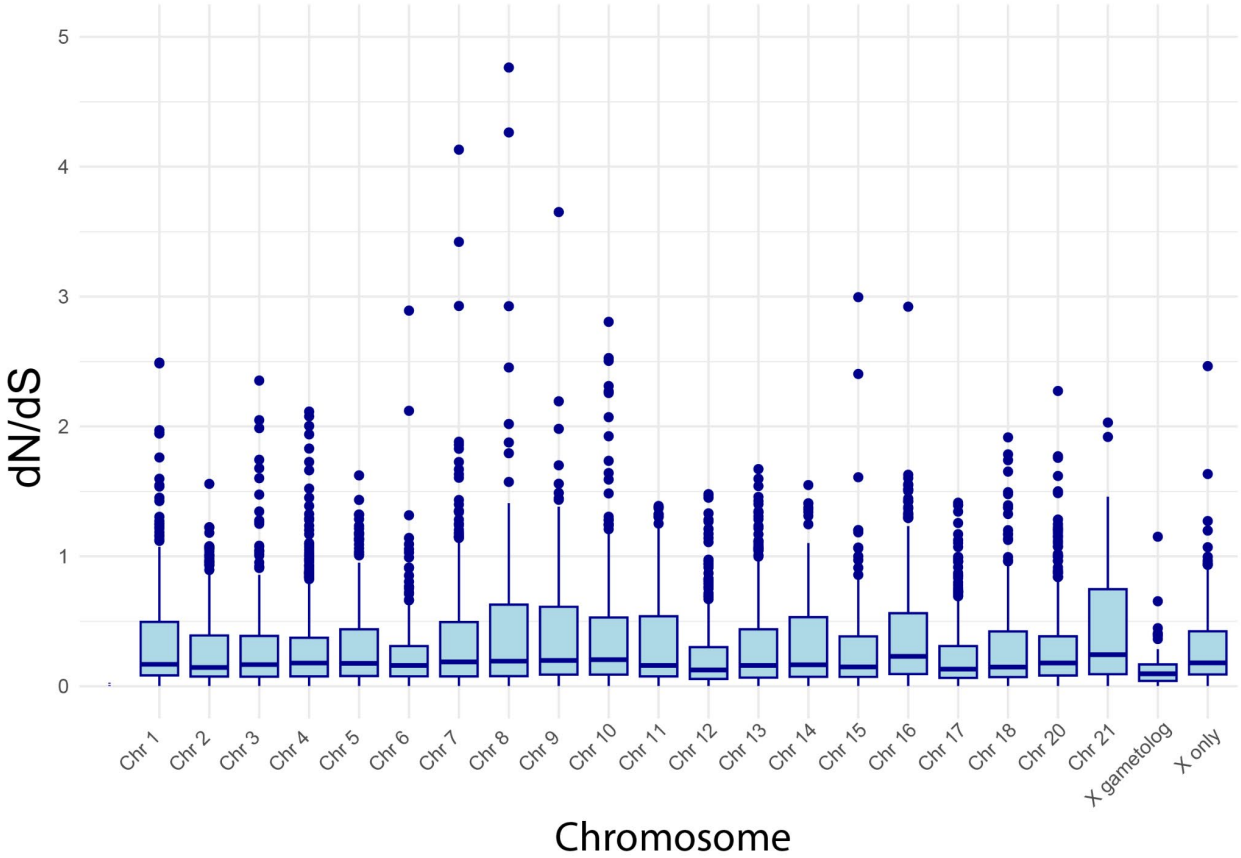

Supplemental Figure 11. d_N/d_S **between threespine and ninespine stickleback for all chromosomes.** Both X gametologs and Chr 12 (Ninespine sex chromosomes) have lower dN/dS than median autosomal ($P < 0.01$, Kruskal Wallis and Dunn's test). All other comparisons are not statistically different ($P > 0.05$ for all pairwise comparisons).

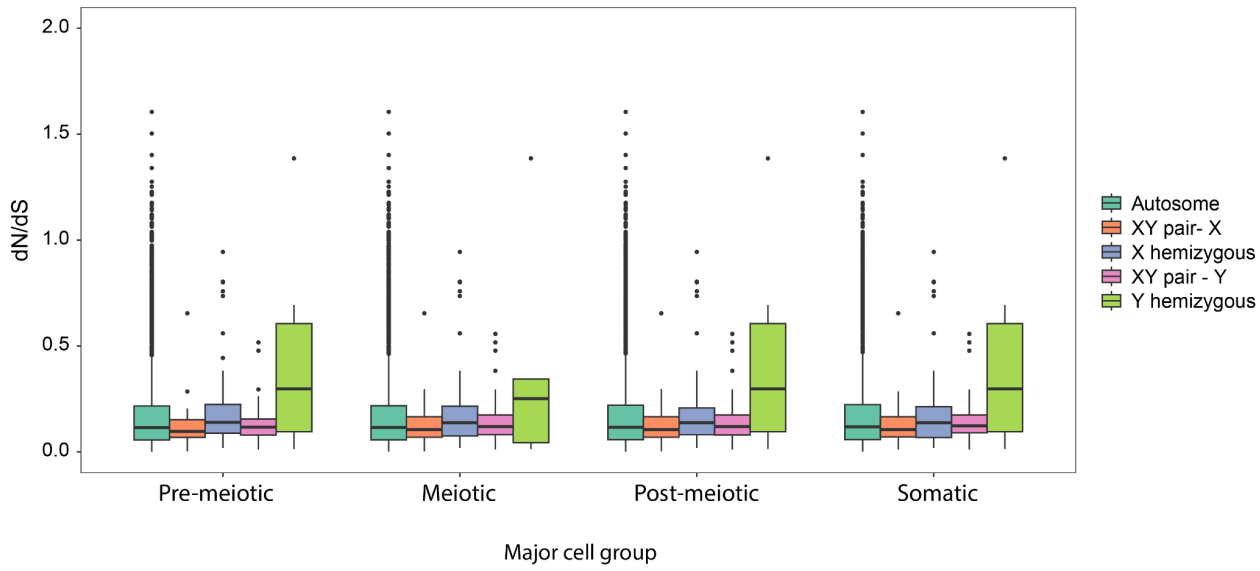

1810

1811

1812 **Supplemental Figure 12. Similar signatures of selection across spermatogenesis.** d_N/d_S was

1813 calculated between ninespine and threespine stickleback for genes on autosomes, X hemizygous

1814 genes, X and Y gametologs, and Y homozygous genes. scRNA-seq was used to identify 2378

1815 genes that were induced in four major cell groups. There were no significant differences between

1816 stages for each chromosome group (P = 0.501 Kruskal Wallis and Dunn's test). The dataset

1817 includes genes that were induced and had an alignment between threespine and ninespine

1818 stickleback cross four developmental stages for each chromosome category. Autosomes have the

1819 largest sample sizes, with 414, 465, 340, and 1,043 genes across the four stages, respectively. X

1820 gametologs include 16, 3, 5, and 7 genes; X-only genes have 24, 9, 9, and 8 genes; Y gametologs

1821 consist of 16, 3, 5, and 7 genes; and Y-only genes are the smallest group, with just 2 genes in

1822 each of the last two stages.

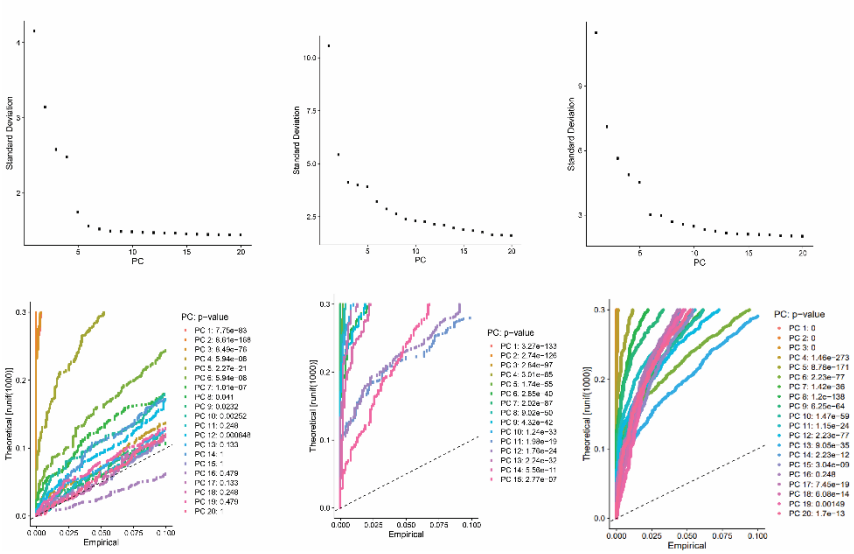

Supplemental Figure 13. Identification of significant principal components for scRNA-seq

Elbow plots and jackstraw simulations were generated to assess the number of significant principle components for each sequencing experiment.

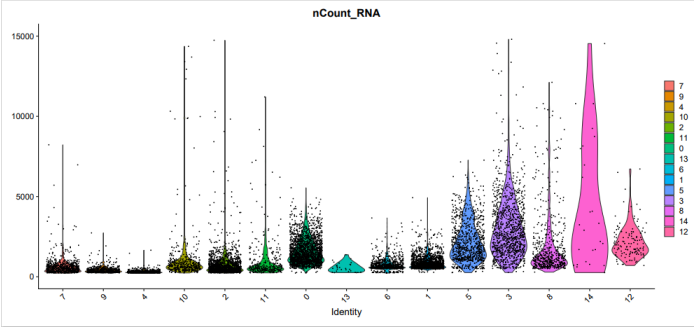

Supplemental Figure 14. Number of reads per cell type.

Number of RNA molecules identified per cell within each cell cluster were counted using Seurat.